Redox Biology 26 (2019) 101287

Contents lists available at ScienceDirect

Redox Biology

journal homepage: www.elsevier.com/locate/redox

Therapeutic contribution of melatonin to the treatment of septic cardiomyopathy: A novel mechanism linking Ripk3-modified mitochondrial performance and endoplasmic reticulum function

Jiankai Zhong[a,b,1], Ying Tan[c,1,**], Jianhua Lu[b], Jichen Liu[a], Xiaochan Xiao[c], Pinji Zhu[d], Sainan Chen[c], Sulin Zheng[b], Yuying Chen[b], Yunzhao Hu[b], Zhigang Guo[a,*]

[a] Department of Cardiology, Huiqiao Medical Center, Nanfang Hospital, Southern Medical University, Guangzhou, 510515, China
[b] Department of Cardiology, Shunde Hospital, Southern Medical University (The First People's Hospital of Shunde Foshan), Foshan, 528308, Guangdong, China
[c] Department of Emergency Medicine, Nanfang Hospital, Southern Medical University, Guangzhou, 510515, China
[d] Medical School of Chinese PLA, PLA General Hospital, Beijing, 100853, China

ARTICLE INFO

Keywords:
Septic cardiomyopathy
Ripk3
Melatonin
Mitochondrial injury
ER stress
Cardioprotective signaling pathways

ABSTRACT

The basic pathophysiological mechanisms underlying septic cardiomyopathy have not yet been completely clarified. Disease-specific treatments are lacking, and care is still based on supportive modalities. The aim of our study was to assess the protective effects of melatonin on septic cardiomyopathy, with a focus on the interactions between receptor-interacting protein kinase 3 (Ripk3), the mitochondria, endoplasmic reticulum (ER) and cytoskeletal degradation in cardiomyocytes. Ripk3 expression was increased in heart samples challenged with LPS, followed by myocardial inflammation, cardiac dysfunction, myocardial breakdown and cardiomyocyte death. The melatonin treatment attenuated septic myocardial injury in a comparable manner to the genetic depletion of Ripk3. Molecular investigations revealed that Ripk3 intimately regulated mitochondrial function, ER stress, cytoskeletal homeostasis and cardioprotective signaling pathways. Melatonin-mediated inhibition of Ripk3 improved mitochondrial bioenergetics, reduced mitochondria-initiated oxidative damage, sustained mitochondrial dynamics, ameliorated ER stress, normalized calcium recycling, and activated cardioprotective signaling pathways (including AKT, ERK and AMPK) in cardiomyocytes. Interestingly, Ripk3 overexpression mediated resistance to melatonin therapy following the infection of LPS-treated hearts with an adenovirus expressing Ripk3. Altogether, our findings identify Ripk3 upregulation as a novel risk factor for the development of sepsis-related myocardial injury, and melatonin restores the physiological functions of the mitochondria, ER, contractile cytoskeleton and cardioprotective signaling pathways. Additionally, our data also reveal a new, potentially therapeutic mechanism by which melatonin protects the heart from sepsis-mediated dysfunction, possibly by targeting Ripk3.

1. Introduction

Septic shock, which is caused by a serious inflammatory response, is the leading cause of mortality and morbidity in hospitalized patients worldwide [1,2]. Sepsis-induced myocardial injury, a reversible form of cardiac depression, is characterized by cardiomyocyte death, oxidative stress, an excessive inflammatory response, microvascular vasospasms and ventricular systolic disorder [3,4]. In patients with septic shock, elevated hs-cTnI levels, decreased cardiac output, increased peripheral vascular resistance and cool extremities are noted in clinical practice [5,6]. Additionally, the majority of patients with septic cardiomyopathy exhibit increased early, but not late, mortality, as well as postdischarge cardiovascular morbidity [7,8]. Accordingly, an effective and rapid therapeutic approach to attenuate septic cardiomyopathy remains an urgent clinical need [9].

At the cellular level, cardiomyocytes are the primary target that undergo death during septic cardiomyopathy due to excess inflammation [10]. At the molecular level, two signaling pathways are altered in answer to septic shock: mitochondrial injury and endoplasmic reticulum (ER) stress [11,12]. The mitochondrion is an energy center of

* Corresponding author.
** Corresponding author.
E-mail addresses: tanying1115@163.com (Y. Tan), guozhigang126@126.com (Z. Guo).
[1] Jiankai Zhong and Ying Tan contributed equally to this work.

https://doi.org/10.1016/j.redox.2019.101287
Received 22 June 2019; Received in revised form 9 July 2019; Accepted 26 July 2019
Available online 27 July 2019
2213-2317/ © 2019 The Authors. Published by Elsevier B.V. This is an open access article under the CC BY-NC-ND license (http://creativecommons.org/licenses/BY-NC-ND/4.0/).

the cardiomyocyte, controlling cardiomyocyte metabolism and survival by constantly providing ATP [13,14]. The ER is the internal calcium store, supporting cardiomyocyte contractile and relaxation functions by tightly recycling cytoplasmic calcium concentrations [15,16]. Numerous investigations have provided insights into the causal roles of mitochondrial injury and ER stress in the progression of septic cardiomyopathy [17,18]. However, the upstream mediator of mitochondrial damage and ER dysfunction has not been identified.

Recently, receptor-receptor-interacting protein kinase 3 (Ripk3) activation has been shown to be closely associated with the pathological progression of inflammation [19]. A Ripk3 deficiency attenuates inflammation and organ injury in neonates with sepsis [20]. Mechanistically, Ripk3 enhances sepsis-induced kidney injury via promoting mitochondrial dysfunction [21]. This finding is subsequently supported by an observation in a cardiac ischemia reperfusion model that genetic ablation of Ripk3 reduces cardiomyocyte death through modulating mitochondrial homeostasis [22]. Additionally, the relationship between Ripk3 activation and ER stress has also been identified in breast cancer and cardiac hypertrophy [23]. Thus, Ripk3 seems to be the common upstream signal for mitochondrial injury and ER stress [24,25]. Accordingly, investigations of whether Ripk3 participates in septic cardiomyopathy by affecting both mitochondrial injury and ER stress would further benefit the field.

Despite the numerous studies performed to date, very few therapies are available for inflammation-induced cardiac depression [26,27]. Melatonin, a product of tryptophan, modulates the inflammatory response, cell apoptosis [28], oxidative stress, and microvascular vasospasms [29] in various disease models, such as cardiac ischemia reperfusion injury [30], fatty liver disease [31], drug-induced acute renal injury [32], Parkinson's disease, and cancer. The therapeutic effects of melatonin on sepsis have also been widely explored and several protective mechanisms of melatonin have been proposed. Activation of the PI3K/Akt pathway, inhibition of the NLRP3 inflammasome, and antioxidant properties have been identified as the regulatory mechanisms that explain the beneficial effect of melatonin on sepsis. Melatonin was recently shown to prevent Ripk3 activation and subsequently send prosurvival signals to the reperfused heart [22]. However, no evidence is available that establishes the effect of melatonin on Ripk3 in the setting of septic cardiomyopathy. Moreover, in light of the protective effects of melatonin on the mitochondria and ER, studies exploring the therapeutic potential of targeting the Ripk3-modified mitochondrial injury and ER stress with melatonin in animal models of lethal septic cardiomyopathy are worthwhile. Collectively, the goals of our study are to verify 1) whether Ripk3 is upregulated in septic cardiomyopathy; 2) whether increased Ripk3 expression enhances cardiac depression by inducing mitochondrial injury and ER stress; and 3) whether melatonin reverses septic cardiomyopathy by suppressing Ripk3 activation, improving mitochondrial performance and normalizing ER function.

2. Materials and methods

2.1. Animals and treatment

All experimental protocols were approved by the Animal Experiment Committee of Nanfang Hospital at Southern Medical University (Guangzhou, China). Male C57BL/6 wild-type (WT) mice and Ripk3-knockout (Ripk3-KO) mice were purchased from GemPharmatech. These mice, weighing 20 g–22 g (10–12 weeks old), had free access to food and water and were housed at 26 °C on a normal light/dark cycle. A septic cardiomyopathy model was established via an intraperitoneal injection of 15 mg/kg LPS [33,34]. The concentration was selected based on a previous study using a model of septic cardiac cardiomyopathy. Forty-eight hours after the injection, cardiac function was analyzed (n = 6 per group). The hearts of the mice in each group were immediately collected for further assays. Melatonin (20 mg/kg; Sigma-Aldrich, St. Louis, MO, USA) was intraperitoneally injected 12 h before LPS-induced myocardial injury. To reactivate Ripk3 in melatonin-treated mice, the adenoviral vector expressing Ripk3 (ad-Ripk3) was injected into the myocardium of melatonin-treated mice 24 h before LPS injury, as described in a previous study [22].

2.2. Cell culture

Primary cardiomyocytes were isolated from WT and Ripk3-KO mice using an enzyme digestion method described in a previous study [35]. Cardiomyocytes were cultured in Dulbecco's modified Eagle's medium (DEME) supplemented with 20% fetal bovine serum (FBS), 100 U/ml penicillin and 100 mg/ml streptomycin at 37 °C in a humidified atmosphere with 5% CO_2 and maintained in a logarithmic growth phase for all experiments [36]. LPS (5 μg/ml) was added to the cultures for 48 h to induce cardiomyocyte damage, and 10 μM melatonin was used to protect cardiomyocytes from LPS-induced inflammatory injury [37].

2.3. Echocardiography and cardiomyocyte shortening/relengthening evaluations

Echocardiography was performed on all mice using an Esaote Twice System with an SL3116 transducer [38]. Two-dimensional and M-mode echocardiographic measurements were recorded with a VEVO 2100 high-resolution *in vivo* imaging system [39]. Cardiomyocyte shortening and relengthening assays were performed using a SoftEdge MyoCam system (IonOptix, Milton, MA), as described in a previous study [40]. Briefly, cardiomyocytes were isolated from reperfused hearts, and then single cardiomyocytes were observed under an inverted microscope. The time to peak shortening (TPS), time to 90% relengthening (TR90), maximal velocity of shortening (+dL/dt), and maximal velocity of relengthening (-dL/dt) were recorded [41].

2.4. ELISA

The levels of inflammation markers, including interleukin 6 (IL-6), interleukin 10 (IL-10), MCP1, MMP9 and tumor necrosis factor-α (TNF-α) were examined using ELISA kits according to the manufacturer's recommendations [42]. Additionally, the levels of antioxidants such as SOD, GPX and GSH in cardiomyocytes were also detected via ELISAs supplied by Beyotime Biotechnology Co., Ltd. (Beijing, China) [43]. Serum levels of creatine kinase, lactate dehydrogenase (LDH) and troponin T were measured using commercial kits according to the manufacturer's protocols (CUSABIO, Wuhan, China) [44].

2.5. Construction and transfection of the Ripk3 adenoviral vector (ad-Ripk3)

For stable overexpression of Ripk3 in cardiomyocytes, a Ripk3 adenoviral vector was designed and generated by Obio Technology (Shanghai, China) [45]. The plasmids were also extracted and sequenced by Obio Technology. Cardiomyocytes were transfected with the Ripk3 adenoviral vector using a ViraDuctin™ Transduction Kit [46]. After 48 h of incubation in a 5% CO_2 incubator, the transfection was terminated, and western blotting was used to confirm the overexpression efficiency [47].

2.6. Western blotting

Samples were washed with pre-cooled PBS, lysed in RIPA solution, and centrifuged at 12,000 × *g* for 30 min. Following detection of protein concentration by BCA (Beyotime Biotechnology, Beijing, CHINA), proteins (30 μg) were separated by 10% sodium dodecyl sulfatepolyacrylamide (SDS-PAGE) gel electrophoresis and transferred onto a polyvinylidene difluoride (PVDF) membrane [48]. After blocking the nonspecific binding sites with 5% non-fat milk in Tris buffered saline-Tween 20 (TBS-T), the membranes were incubated overnight with

antibodies against Drp1 (1:1000, Abcam, #ab56788), Opa1 (1:1000, Abcam, #ab42364), Mfn2 (1:1000, Abcam, #ab56889), Mff (1:1000, Cell Signaling Technology, #86668), Beclin1 (1:1000, Cell Signaling Technology, #3738), Parkin (1:1000, Cell Signaling Technology, Inc.), JNK (1:1,000; Cell Signaling Technology, #4672), p-JNK (1:1,000; Cell Signaling Technology, #9251), SERCA (1:1000, Cell Signaling Technology, Inc.), AMPK (1:1000, Abcam, #ab131512), p-AMPK (1:1000, Abcam, #ab23875), Mst1 (1:1000, Cell Signaling Technology, #3682), t-Akt (1:1000, Abcam, #ab8805), p-Akt (1:1000, Abcam, #ab81283), p-ERK (1:1000, Abcam, #ab176660), t-ERK (1:1000, Abcam #ab54230), PERK (1:1000, Abcam, #ab79483), CHOP (1:1000, Abcam, #ab179823), GRP78 (1:1000, Abcam, #ab21685), IP3R (1:1000, Abcam, #ab5804) at 4 °C overnight [49]. The membranes were washed with TBS-T and incubated with goat anti-rabbit IgG, peroxidase conjugated secondary antibodies (1:5,000, Biosharp Life Sciences, China) at room temperature for 1 h [50]. Proteins were visualized using chemiluminescence detection reagents (Thermo Scientific Pierce ECL Plus). Relative band intensities were determined by Image Lab software (Bio-Rad Technologies) [51]. GAPDH was used as an internal control. The results of analysis were expressed as a relative ratio of the target protein to internal reference. All experiments were repeated three times [52].

2.7. Immunofluorescence

The immunofluorescence studies were carried out as described previously. Briefly, cultured cardiomyocytes or heart tissues were fixed with 4% paraformaldehyde, incubated in 3% normal donkey serum containing 0.3% Triton X-100 at 37 °C for 1 h [53], and incubated with primary antibodies overnight at 4 °C, followed by incubation with secondary antibodies. Then, the samples were stained with DAPI and observed and captured using an Olympus FV1000 (Olympus, Tokyo, Japan) laser confocal microscope [54]. The images were analyzed using Image Pro-Plus software (Image Solutions, Torrance, CA, USA). The primary antibodies used in the present study were as follows: p-Akt (1:1000, Abcam, #ab81283), p-JNK (1:1,000; Cell Signaling Technology, #9251), Tom20 (1:1,000, Abcam, #ab186735), Myosin (1:1000, Abcam, #ab50967), tubulin (1:1000, Cell Signaling Technology, #5335), Gr1 (1:1000, Abcam, #ab25377), troponin T (1:1000, Abcam, #ab8295), cleaved caspase3 (1:1000, Abcam, #ab49822) [55].

2.8. Electron microscopy

After treatment and injury, tissues were immediately isolated from the left ventricle and fixed with 2% glutaraldehyde at 4 °C for 30 min. Thin sections (60 nm) were then cut and stained with lead citrate and uranyl acetate at room temperature for 4 h. Next, samples were embedded in resin at room temperature for another 2 h. A Hitachi H600 Transmission Electron Microscope (Hitachi, Ltd., Tokyo Japan) was used to observe the samples [56].

2.9. Mitochondrial oxygen consumption rate (OCR) and mitochondrial membrane potential detection

An ATP Bioluminescence Assay Kit was used to analyze cellular ATP production as described in a previous report. The mitochondrial oxygen consumption rate (OCR) was evaluated with an XFe96 extracellular flux analyzer (Agilent Technologies, CA, USA) [57]. Mitochondrial membrane potential was determined via JC-1 probe (Molecular Probe, USA) according to the manufacture's instruction [58].

2.10. MTT assay and LDH release assay

Cell viability was determined using a routine MTT assay. Briefly, cardiomyocytes were seeded in 96-well plates at a density of 1×10^4 cells/well [59]. After treatment with LPS and/or melatonin, the media were removed and replaced with 10 μl of the MTT solution (5 mg/ml). After a 3 h incubation, the MTT was removed and 150 μl of DMSO were added to each well. The optical density was recorded at 570 nm (OD570) using a microplate reader (MK3, Thermo, Germany). The LDH release assay was performed using a commercial kit (Beyotime Biotechnology, Beijing, China) [60].

2.11. Flow cytometry analysis of mitochondrial ROS production

Cardiomyocytes were seeded onto 6-well plates and then treated with LPS and melatonin to detect mitochondrial ROS production [61]. Next, cells were pretreated with the MitoSOX red mitochondrial superoxide indicator (Molecular Probes, USA) at a final concentration of 10 μM at 37 °C for 30 min, as described in a previous study [62]. Then, cells were harvested and resuspended in PBS. The mitochondrial ROS level was detected using fluorescence spectroscopy [63].

2.12. TUNEL staining and detection of cardiomyocyte calcium concentrations

Cell death was identified using the terminal deoxynucleotidyl transferase-mediated dUTP nick-end labeling (TUNEL) assay with an in situ Cell Death Detection kit (Promega, Madison, WI, USA), according to the manufacturer's instructions [64,65]. Five fields per section in three sections were examined from each experimental group. Fura-2-AM (Molecular Probes) was used to detect the intracellular calcium concentration, and cellular calcium was subsequently performed under an inverted microscope. The fluorescence intensity of calcium was measured using Image Pro-Plus software (Image Solutions, Torrance, CA, USA) [66].

2.13. qRT-PCR

Total RNA was extracted from harvested cells using TRIzol reagent (Thermo Fisher Scientific, Inc.). RNA was quantified and reverse-transcribed into complementary DNAs using specific stem-loop reverse transcription primers [67]. First-strand mRNAs were synthesized using a HiScript II Q RT SuperMix for qPCR (Vazyme Biotech Co, Ltd.), and the quantitative real-time PCR analysis (qRT-PCR) was performed using a ChamQTM Universal SYBR qPCR Master Mix (Vazyme Biotech Co., Ltd.) on a Bio-Rad CFX96TM R-T PCR instrument (Bio-Rad) [68]. The Vazyme cycling conditions were: 95 °C for 30 s followed by 39 cycles at 95 °C for 10 s and 60 °C for 30 s. Then, a melting curve analysis was performed by increasing the temperature 0.5 °C from 65 °C to 95 °C for 15 min. GAPDH was used as a loading control. PCR primers used in this study were synthesized by Sangon Biotech (Shanghai, China) and the sequences were: TNFα (Forward, 5'-AGATGGAGCAACCTAAGGTC-3'; Reverse, 5'-GCAGACCTCGCTGTTCTAGC-3'), MCP1 (Forward, 5'-GGA TGGATTGCACAGCCATT-3'; Reverse, 5'-GCGCCGACTCAGAGGTGT-3'), and IL1 (Forward, 5′-TTGCTCGAGTGAGTGAGGAT-3′, Reverse, 5′-TGTGACAGCGATGGACAGTG-3′) [69].

2.14. Statistical analysis

Data were generated through at least three independent experiments and were presented as the means ± SEM. The statistical analyses were performed using SPSS 16.0 (SPSS, Inc., Chicago, IL, USA). All results in the present study were obtained by one-way analysis of variance, followed by Tukey's test. $P < 0.05$ was considered statistically significant.

3. Results

3.1. Ripk3 deletion prevents LPS-induced inflammation and myocardial injury

In the present study, LPS was used to induce sepsis and myocardial

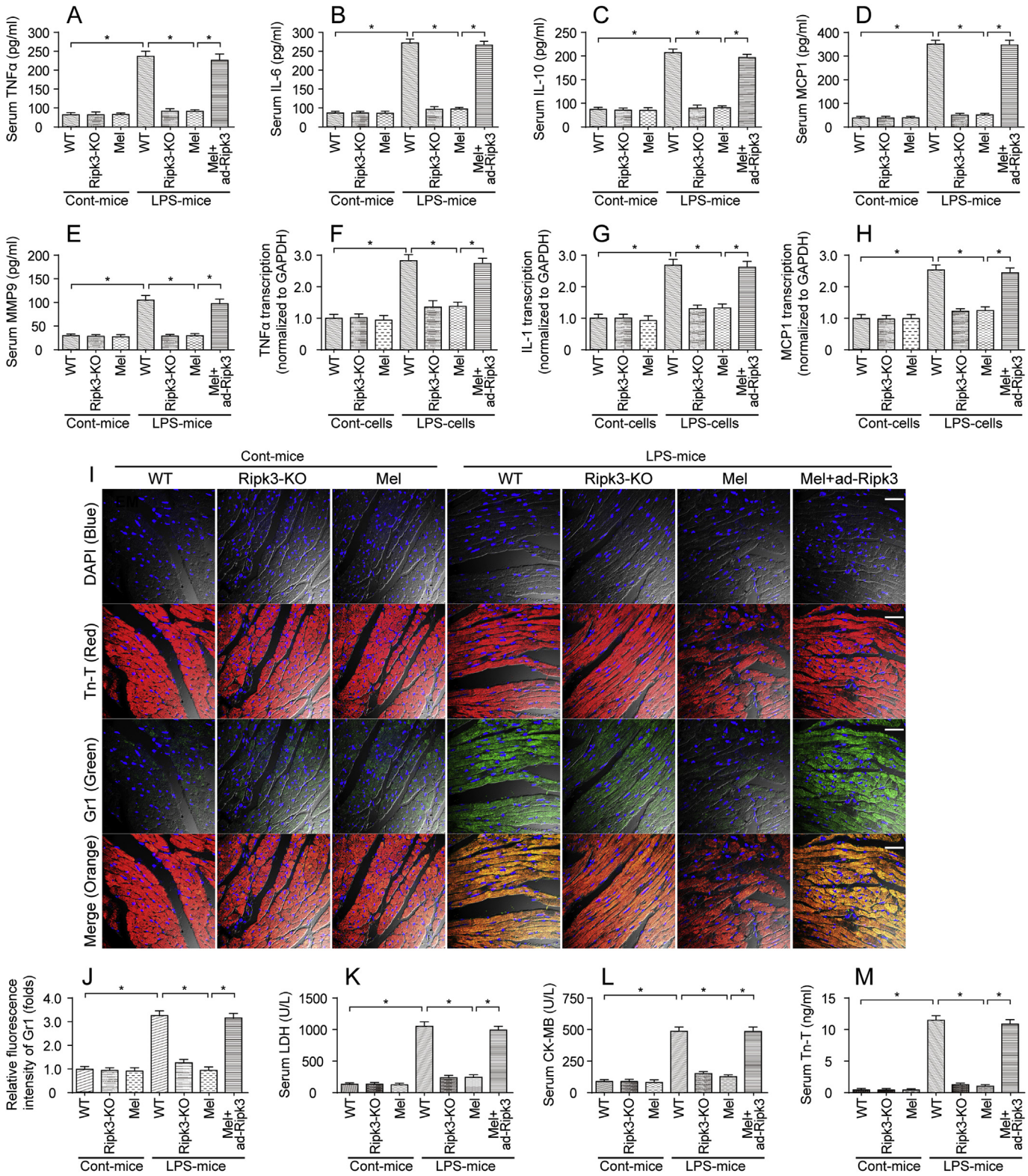

Fig. 1. Melatonin attenuates sepsis-related myocardial inflammation and injury. A-E. LPS was injected into WT and Ripk3-knockout (Ripk3-KO) mice to establish the septic cardiomyopathy model. Then, melatonin was used to prevent LPS-mediated sepsis. Adenovirus-loaded Ripk3 (ad-Ripk3) was injected into melatonin-treated hearts to reverse the suppression of Ripk3 expression in melatonin-treated mice. Subsequently, blood was isolated and ELISAs were used to detect the alterations in TNFα, IL-6, IL-10, MCP-1 and MMP9 levels. **F–H.** After LPS-mediated septic cardiomyopathy, qPCR was used to measure the levels of mRNAs encoding inflammatory factors, such as TNFα, IL-1 and MCP1. **I-J.** Heart tissues were collected and then immunofluorescence staining was performed to analyze the accumulation of Gr-1-positive cells in the myocardium. Tn-T was used to label the myocardial fibers. **K-M.** After the LPS injection, the concentrations of the cardiac damage markers LDH, CK-MB and Tn-T were determined using ELISAs. $^*p < 0.05$. Bar: 120 μm.

injury. An excessive inflammatory response has been acknowledged as the hallmark of septic cardiomyopathy, and therefore, ELISA was used to detect alterations in the serum levels of inflammatory factors. As shown in Fig. 1A–E, compared to the control group, the LPS treatment significantly increased the serum levels of TNFα, IL-6, IL-10, MCP1 and MMP9. Interestingly, the melatonin treatment prevented the increase in the levels of the inflammatory factors, suggesting that melatonin inhibited LPS-induced inflammation. Ripk3 knockout (Ripk3-KO) mice were used to verify whether Ripk3 was involved in LPS-induced sepsis. Additionally, a Ripk3 adenovirus (ad-Ripk3) was infected into the hearts of melatonin-injected mice to induce Ripk3 overexpression and to validate whether melatonin inhibited LPS-induced septic cardiomyopathy via Ripk3. As shown in Fig. 1A–E, compared to the LPS group, Ripk3 deletion significantly reduced the levels of inflammatory factors, similar to the results obtained in animals treated with melatonin. Interestingly, the ad-Ripk3 injection abolished the inhibitory effect of melatonin on the inflammatory response. This finding was further supported by results obtained from cardiomyocytes *in vitro* using qPCR. Compared to the normal cardiomyocytes (Fig. 1F–H), the LPS treatment increased the levels of transcripts encoding inflammatory factors, including TNFα, IL-1 and MCP1. Interestingly, the melatonin treatment decreased the levels of the transcripts encoding inflammatory factors; this effect was negated by ad-Ripk3 transfection (Fig. 1F–H).

Then, immunofluorescence staining was used to observe myocardial inflammation in response to LPS treatment and/or melatonin supplementation. As shown in Fig. 1I–J, compared to the control group, the LPS treatment increased the immunofluorescence intensity of Gr1, a surface marker of neutrophils. Interestingly, Ripk3 deletion and/or melatonin treatment reduced Gr1 expression in LPS-treated hearts. However, ad-Ripk3 transfection abolished the regulatory effect of melatonin on $Gr1^+$ neutrophil accumulation (Fig. 1I–J). Subsequently, myocardial inflammation and injury were further evaluated via analyzing the levels of cardiac damage markers using ELISAs. In response to the LPS treatment, the levels of cardiac damage markers, such as LDH, troponin T (Tn-T) and CK-MB, were rapidly increased by LPS stress and were reversed to near-normal levels after treatment with melatonin (Fig. 1K-M); the beneficial effects of melatonin were neutralized by ad-Ripk3 transfection. Based on these results, LPS-induced septic cardiomyopathy appeared to be associated with Ripk3 upregulation, and melatonin attenuated LPS-induced myocardial inflammation and injury by reducing Ripk3 expression.

3.2. The inhibitory effect of melatonin on Ripk3 sustains heart function

An excessive inflammatory response would impair heart function. Therefore, echocardiography was used to detect alterations in heart function upon exposure to LPS. As shown in Fig. 2A–D, compared to the control group, the left ventricular ejection fraction (LVEF), fractional shortening (LVFS) and left ventricular end systolic pressure (LVESP) were decreased in response to the LPS treatment. In contrast, the left ventricular end-diastolic pressure (LVEDP) were increased in LPS-treated mice. Interestingly, Ripk3 deletion and/or melatonin treatment reversed the changes in cardiac function induced by LPS (Fig. 2A–D); the effect of melatonin was abolished by ad-Ripk3 transfection. Subsequently, cardiomyocytes were isolated from LPS-treated mice and the cardiomyocyte mechanical parameters were monitored to further analyze the changes in cardiomyocyte contractile properties. As shown in Fig. 2E–J, compared to the control group, the LPS treatment had no effect on cardiomyocyte length. Interestingly, cardiomyocytes isolated from LPS-treated mice exhibited reduced peak shortening, an effect that occurred concomitantly with a decrease in the maximal velocity of shortening (+dL/dt) and the maximal velocity of relengthening (-dL/dt). Additionally, LPS-treated cardiomyocytes also displayed an increased time-to-90% relengthening (TR90) and time-to-shortening (TPS). Thus, LPS impaired the contractile and diastolic functions of cardiomyocytes (Fig. 2E–J). Notably, genetic ablation of Ripk3 and/or the melatonin treatment improved the mechanical parameters of cardiomyocyte, despite treatment with LPS, and the beneficial effects of melatonin were abolished by ad-Ripk3 transfection. Taken together, melatonin improved LPS-induced cardiac dysfunction via inhibiting Ripk3 expression.

3.3. LPS-mediated degradation of the cardiomyocyte contractile cytoskeleton is reversed by melatonin

A well-structured cardiomyocyte contractile cytoskeleton is a prerequisite for the contractile function of the heart. Moreover, cytoskeletal degradation is an early event in cardiomyocyte dysfunction and/or death [70]. Therefore, immunofluorescence staining was used to observe the alterations in the cardiomyocyte contractile cytoskeleton in response to the LPS treatment *in vitro*. As shown in Fig. 3A–C, compared to the control group, the fluorescence intensity of Myosin was significantly decreased in response to LPS treatment (white arrows), indicating cytoskeletal degradation. Interestingly, the melatonin treatment reversed the changes in Myosin expression, and this effect was negated by ad-Ripk3 transfection. To verify whether cardiomyocyte contractile cytoskeleton was specifically modulated by melatonin, tubulin, a component of the noncontractile cytoskeleton, was costained in cardiomyocytes. Interestingly, neither melatonin nor LPS altered tubulin levels (Fig. 3A–C), reconfirming that the cardiomyocyte contractile cytoskeleton is specifically modulated by melatonin in the setting of LPS-induced septic cardiomyopathy. Additionally, electron microscopy was used to observe the alterations in the cardiac ultrastructure *in vivo*. As shown in Fig. 3D, compared to the control mice, myocytes from the septic hearts lost the majority of t-tubules and their regular striated pattern. Moreover, the Z line disappeared and myocardial fibers had degraded in LPS-treated mice (red arrows in Fig. 3D). Interestingly, the melatonin treatment maintained the heart ultrastructure by suppressing Ripk3 expression (yellow arrows in Fig. 3D). Accordingly, the above results verify the necessary role of melatonin in maintaining the cardiomyocyte contractile cytoskeleton in the context of LPS-induced septic cardiomyopathy.

3.4. Melatonin reduces cardiomyocyte death in LPS-induced septic cardiomyopathy

Ripk3 is associated with cell death via either apoptosis or necroptosis. In the present study, the TUNEL assay was used to detect cardiomyocyte death *in vivo*. As shown in Fig. 4A–B, compared to the control group, LPS-treated mice exhibited an increased percentage of TUNEL-positive cardiomyocytes. However, the loss of Ripk3 and/or treatment with melatonin reduced the LPS-induced cardiomyocyte death. Notably, ad-Ripk3 transfection abolished the pro-survival effect of melatonin on LPS-treated hearts. This finding was also supported by the results from *in vitro* experiments using an MTT assay and the LDH release assay. As shown in Fig. 4C, compared to the control group, the LPS treatment reduced the viability of cardiomyocytes, as assessed by MTT assay, an effect that was followed by an increase in LDH release into the cardiomyocyte medium (Fig. 4D) and indicates cell death in response to the LPS treatment. Interestingly, the loss of Ripk3 and/or treatment with melatonin increased cardiomyocyte viability and reduced cell death (Fig. 4C–D). However, ad-Ripk3 transfection neutralized the protective effect of melatonin on LPS-treated cardiomyocytes.

The TUNEL assay and caspase-3 staining were performed simultaneously *in vitro* using methods described in a previous study [71,72] to determine whether cardiomyocyte death occurred via apoptosis or necroptosis. Apoptotic cardiomyocytes, whose nuclei were stained with TUNEL, displayed increased caspase-3 expression. In comparison, caspase-3 was not activated during necroptosis. As shown in Fig. 4E–G, compared to the control group, the ratios of $TUNEL^+$/caspase-3^+ and $TUNEL^+$/caspase-3^- cardiomyocytes were rapidly increased in response

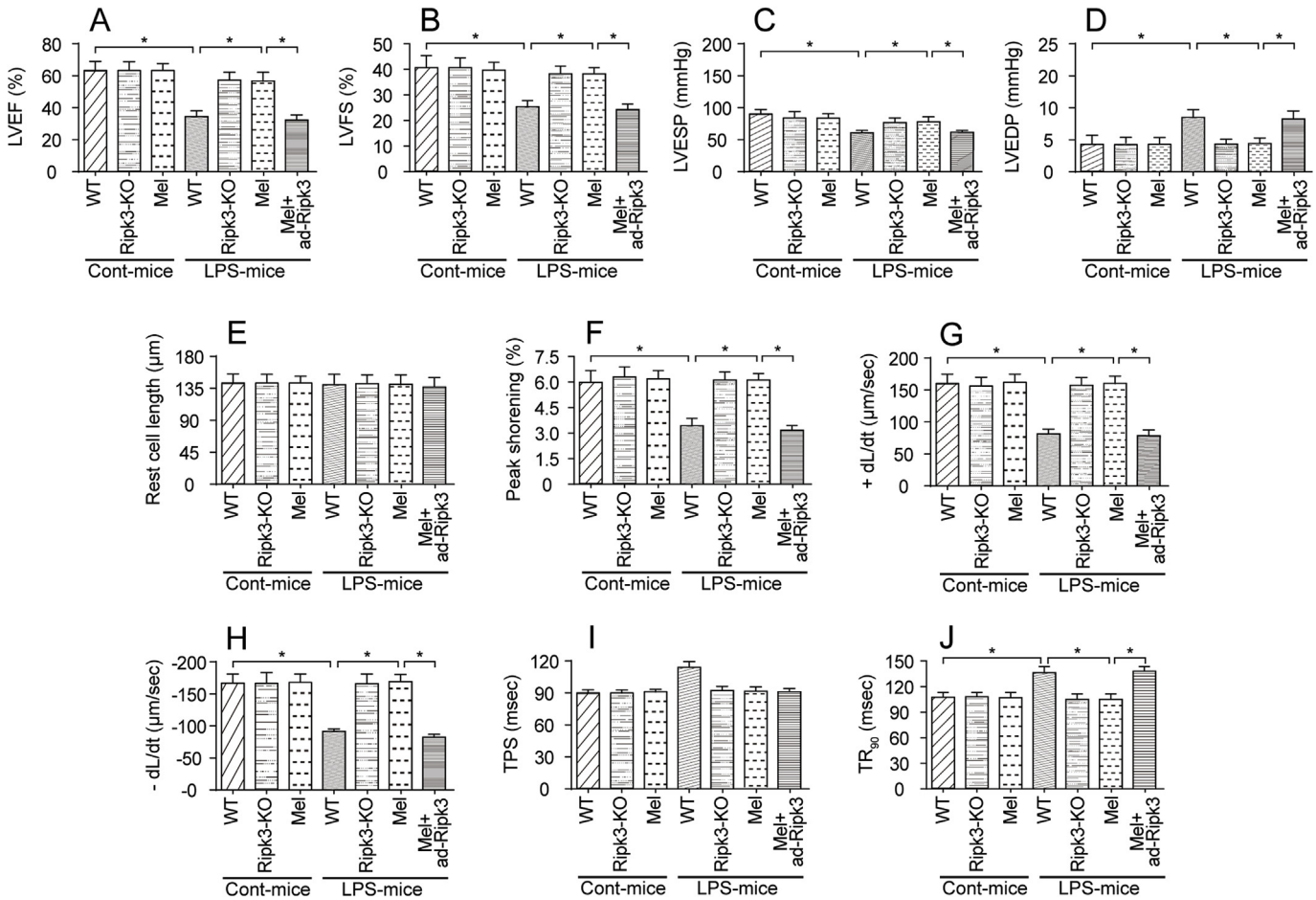

Fig. 2. LPS-mediated septic cardiomyopathy could be improved by melatonin. A-D. Cardiac function was measured using echocardiography. Then, cardiac systolic and diastolic functions were calculated. Melatonin was injected into the LPS-treated hearts. Adenovirus-loaded Ripk3 (ad-Ripk3) was injected into melatonin-treated hearts to reverse Ripk3. **E-J.** Cardiomyocyte mechanical parameters were monitored using a VEVO 2100 high-resolution imaging system. Cardiomyocytes were isolated from LPS-treated mice and melatonin-treated mice. Then, the resting cell length, peak shortening, time-to-90% relengthening (TR90), time-to-shortening (TPS), the maximal velocity of shortening (+dL/dt) and the maximal velocity of relengthening (-dL/dt) were determined. *$p < 0.05$.

to the LPS treatment. Interestingly, a greater number of TUNEL$^+$/caspase-3$^-$ necroptotic cells was observed compared to the TUNEL$^+$/caspase-3$^+$ apoptotic cardiomyocytes (Fig. 4E–G). Based on these results, LPS mediated cardiomyocyte death primarily via necroptosis. Additionally, the melatonin treatment reduced the percentages of TUNEL$^+$/caspase-3$^+$ and TUNEL$^+$/caspase-3$^-$ cells, which was nullified by ad-Ripk3 transfection (Fig. 4E–G). Thus, LPS-induced sepsis was associated with cardiomyocyte death via necroptosis. However, melatonin could maintain cardiomyocyte viability in the setting of septic cardiomyopathy by suppressing Ripk3 expression.

3.5. LPS-activated Ripk3 disturbs mitochondrial bioenergetics and promotes mitochondrial oxidative stress

Previous studies have identified the mitochondrion as the potential candidate organelle contributing to septic cardiomyopathy. At the molecular level, ATP is primarily produced by the mitochondria and assists in the cardiac contractile function [73]. In the present study, the ATP content was significantly decreased in LPS-treated cardiomyocytes (Fig. 5A). However, the Ripk3 deletion and/or melatonin treatment reversed the changes in ATP levels; the effect of melatonin was abrogated by ad-Ripk3 transfection. Subsequently, mitochondrial respiratory function was monitored by determining the oxygen consumption rate (OCR). As shown in Fig. 5B–F, compared to the control group, the baseline OCR, proton leakage, maximal respiratory capacity and ATP turnover were rapidly decreased by LPS. Interestingly, the melatonin treatment reversed the changes in mitochondrial respiration by modulating Ripk3 expression (Fig. 5B–F). This result indicates that mitochondrial bioenergetic is inhibited by LPS due to Ripk3 upregulation and that melatonin maintains mitochondrial energy metabolism in cardiomyocytes by inhibiting Ripk3 expression.

Mitochondrial bioenergetics is closely associated with mitochondrial membrane potential. In Fig. 5G–H, mitochondrial membrane potential, as assessed via JC-1 probe, was reduced in response to LPS treatment and was reversed to near-normal levels with Ripk3 deletion. Similarly, melatonin treatment also stabilized mitochondrial potential in LPS-treated cells and this mitochondrial protective effect of melatonin was negated by Ripk3 overexpression (Fig. 5G–H), suggesting that melatonin modulated mitochondrial potential via suppressing Ripk3. As a consequence of mitochondrial potential reduction, the mitochondria might release ROS into cytoplasm, and increased ROS production is associated with oxidative injury, a component of the pathogenesis of septic cardiomyopathy. Accordingly, mitochondrial ROS overloading was detected using flow cytometry. As shown in Fig. 5I, compared to the control cells, LPS stimulation increased mROS production in cardiomyocytes, and this effect was abolished by melatonin via reducing Ripk3 expression. Subsequently, ELISAs were used to observe the alterations in antioxidant levels. In response to LPS, the levels of SOD, GSH and GPX were decreased in cardiomyocytes (Fig. 5J-L). Interestingly, the melatonin treatment reversed the changes in SOD, GSH and GPX levels by modulating Ripk3 expression (Fig. 5J-L). Thus, LPS also disrupted mitochondrial respiratory function and redox balance, and

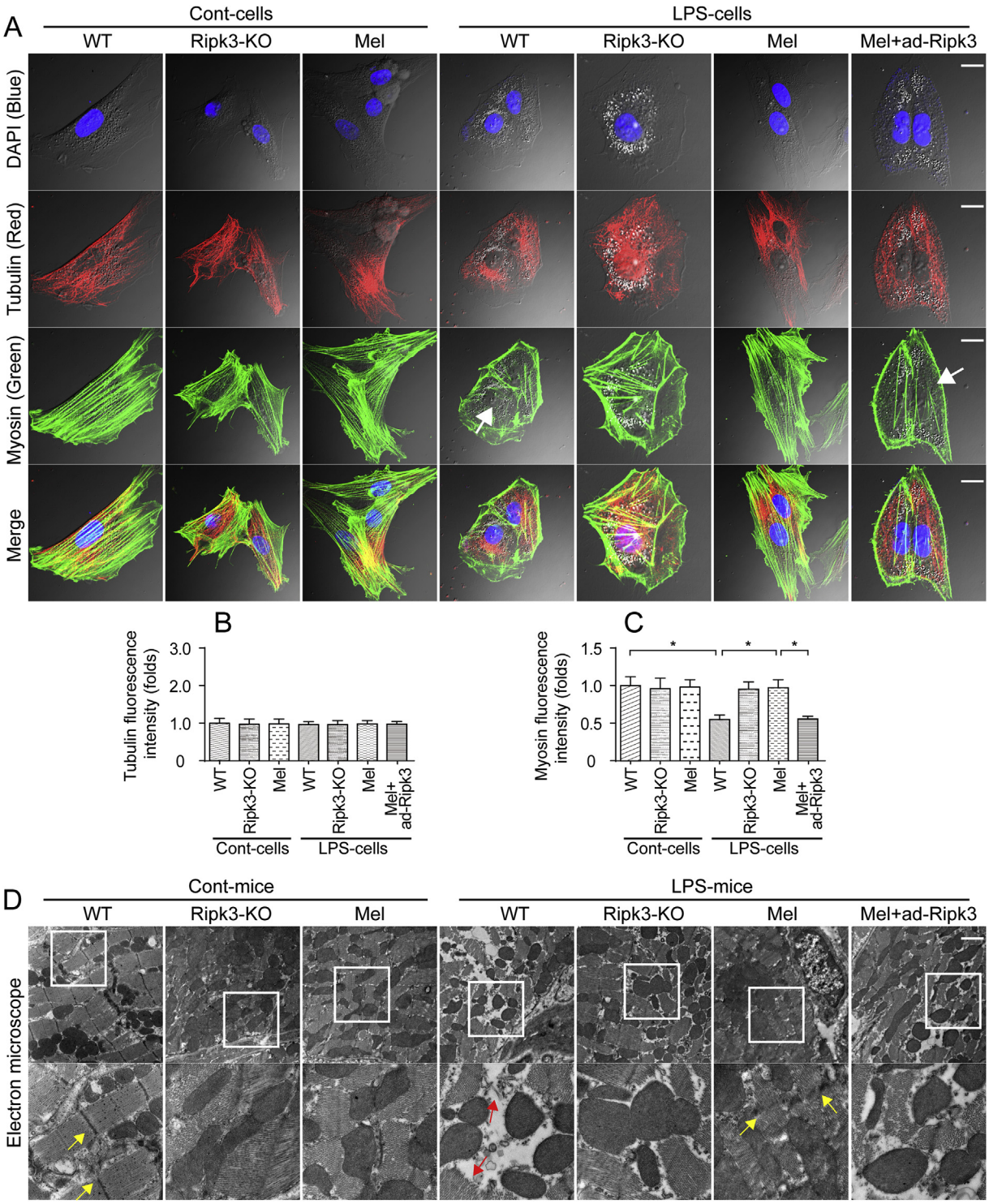

Fig. 3. Melatonin sustained the myocardial contractile cytoskeleton in response to LPS-induced myocardial injury. A-C. Immunofluorescence staining was used to observe the alterations in the cardiac contractile cytoskeleton *in vitro*. A myosin antibody was used to stain the contractile cytoskeleton. Additionally, tubulin, a component of the noncontractile cytoskeleton in cardiomyocytes, was also stained with a tubulin antibody. Then, the fluorescence intensities of myosin and tubulin were measured. White arrows indicate the myosin degratadion. Bar: 35 μm. **D.** Electron microscopy was used to observe the alterations in the structure of the cardiac contractile cytoskeleton *in vivo*. Yellow arrows indicate the Z line in the myocardium. Red arrows indicate the destruction of myocardial fibers. Bar: 2 μm $^*p < 0.05$. (For interpretation of the references to colour in this figure legend, the reader is referred to the Web version of this article.)

these changes were reversed by melatonin through a mechanism depending on Ripk3 suppression.

3.6. Melatonin also modulates mitochondrial dynamics by repressing Ripk3 expression

Recent studies have found that mitochondrial functions, including mitochondrial energy metabolism, mitochondrial calcium homeostasis,

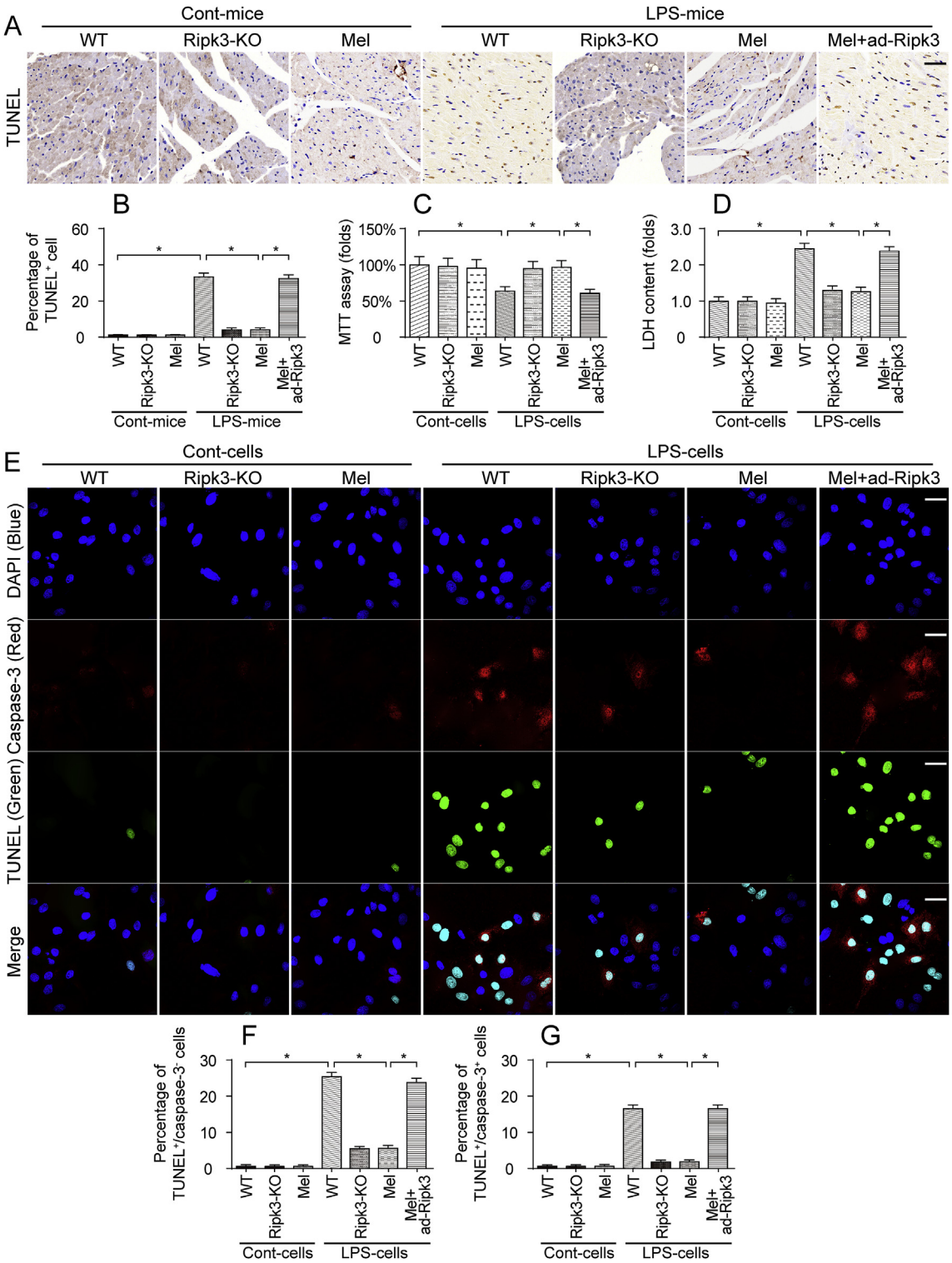

Fig. 4. LPS triggered cardiomyocyte death via necroptosis. A-B. The TUNEL assay was used to evaluate cell death in response to the LPS injection and/or melatonin treatment. The percentage of TUNEL-positive cells was measured. Bar: 180 μm. **C.** Cardiomyocytes were isolated from mice and then treated with LPS or melatonin. Then, cell viability was evaluated using the MTT assay. **D.** After treatment with melatonin and/or LPS, the concentrations of LDH were determined using an ELISA, which was used to monitor cardiomyocyte death in response to LPS stress. **E-G.** *In vitro*, cardiomyocytes were treated with LPS and/or melatonin. Then, the TUNEL assay and cleaved caspase-3 immunofluorescence staining were conducted. The percentage of TUNEL$^+$/cleaved caspase-3$^+$ cardiomyocytes was counted to determine the number of apoptotic cells. Additionally, the number of TUNEL$^+$/cleaved caspase-3$^-$ cardiomyocytes was calculated as the necroptotic cells. Bar: 75 μm *$p < 0.05$.

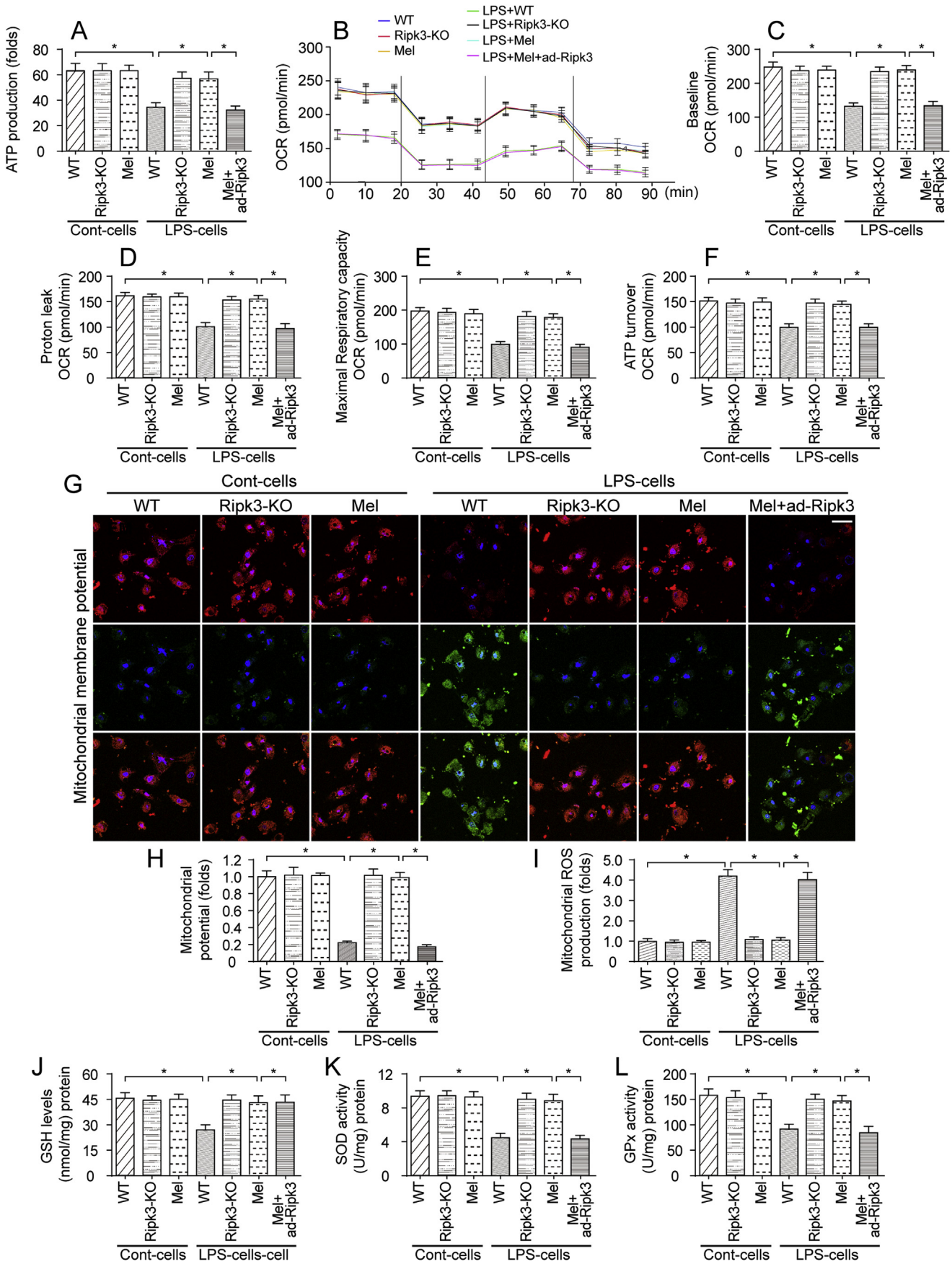

(caption on next page)

Fig. 5. Mitochondrial bioenergetics were negatively modulated by melatonin through a reduction in Ripk3 expression. A. Cardiomyocytes were isolated from WT and Ripk3-KO mice and then treated with LPS. Subsequently, ATP production was measured to reflect mitochondrial energy metabolism. **B–F.** Mitochondrial respiratory function was determined by analyzing the mitochondrial oxygen consumption rate (OCR). The baseline OCR, proton leak OCR, maximal respiratory capacity OCR, and ATP turnover OCR were determined. **G-H.** Mitochondrial membrane potential was measured via JC-1 probe. **I.** Cardiomyocytes were isolated from WT and Ripk3-KO mice. Then, mitochondrial ROS were stained with MitoSOX red, a mitochondrial superoxide indicator, and mitochondrial ROS production was analyzed using flow cytometry. **J-L.** Cardiomyocytes were lysed and then ELISAs were used to determine changes in the levels of the antioxidants GSH, GOD and GPx. $*p < 0.05$. (For interpretation of the references to colour in this figure legend, the reader is referred to the Web version of this article.)

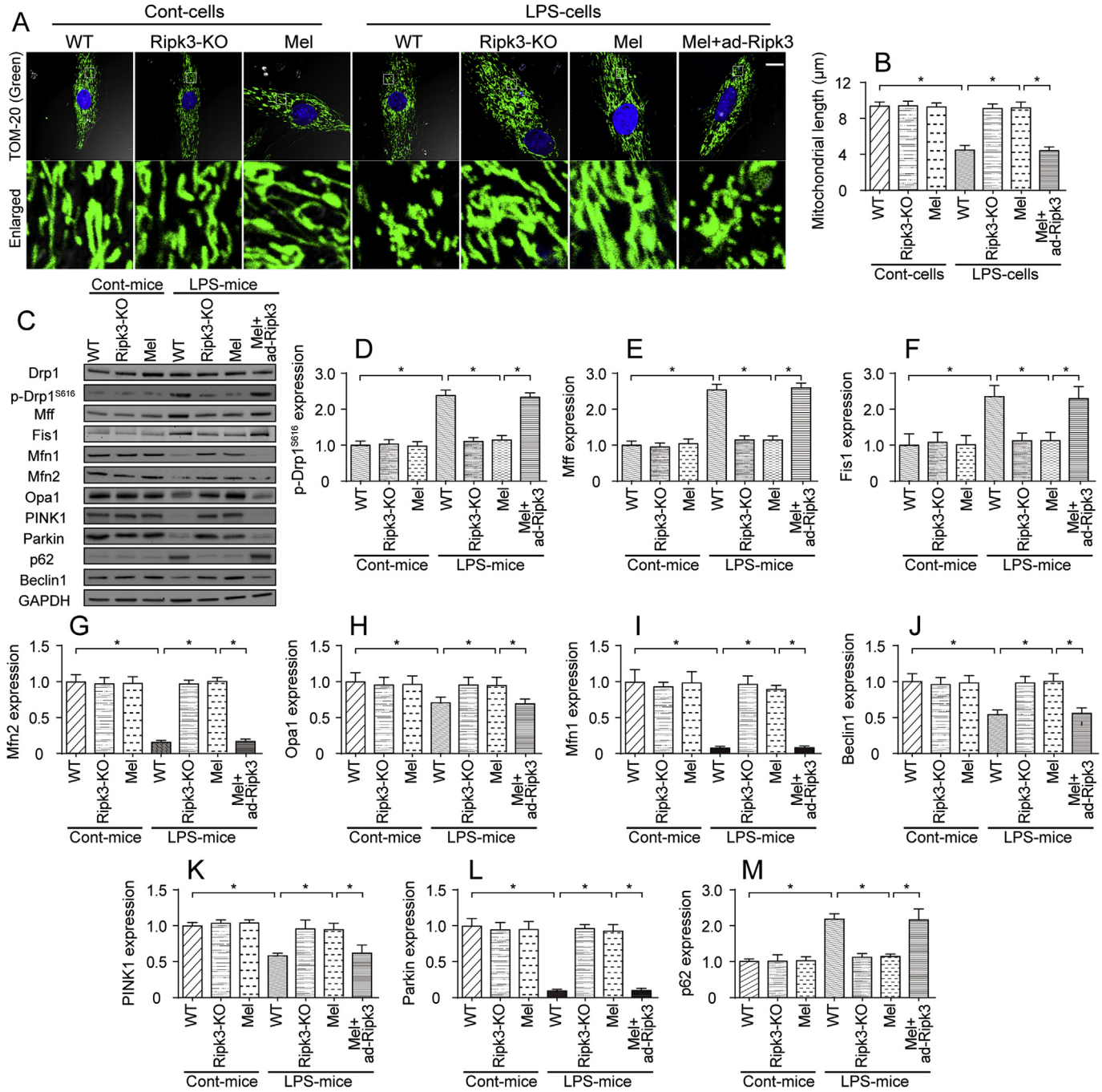

Fig. 6. Mitochondrial dynamics were modified by melatonin in a manner dependent on Ripk3 repression. A-B. Mitochondrial morphology was determined using immunofluorescence staining with a Tom-20 antibody. In response to the LPS treatment, the mitochondria were divided into several fragments, and these alterations were reversed by melatonin. Then, the mitochondrial length was measured in different groups. Bar: 20 μm. **C-M.** Mitochondrial fission factors, mitochondrial fusion parameters, and mitophagy markers were determined using western blotting. Drp1 and Mff were the mitochondrial fission factors. Mfn2 and Opa1 were the mitochondrial fusion parameters. Beclin1 and Parkin were the mitophagy markers. $*p < 0.05$.

mitochondrial oxidative stress and mitochondrial apoptosis, are modulated by mitochondrial dynamics [74–76]. Accordingly, we wanted to determine whether melatonin maintained the mitochondrial energy metabolism and redox balance via regulating mitochondrial dynamics. First, the mitochondrial structure was observed via immunofluorescence staining. As shown in Fig. 6A–B, compared to the control group, the LPS treatment induced the mitochondria to divide into several fragments. The average length of the mitochondria was reduced to ~4.4 μm in cardiomyocytes. Interestingly, the melatonin treatment and/or Ripk3 deletion preserved the mitochondrial structure and increased the mitochondrial length to ~9.2 μm after the LPS treatment. Notably, the transfection of ad-Ripk3 into melatonin-treated cardiomyocytes induced mitochondrial fragmentation, an effect that was accompanied with by a decrease in mitochondrial length (Fig. 6A–B). Based on these results, LPS disturbed mitochondrial dynamics, and melatonin maintained the mitochondrial network via reducing Ripk3 expression.

Subsequently, western blotting was performed to observe mitochondrial dynamics. First, the levels of proteins related to mitochondrial fission (Fig. 6C-I), such as Drp1, Mff and Fis1, were rapidly increased in LPS-treated hearts *in vivo*. Additionally, the levels of mitochondrial fusion factors, such as OPA1, Mfn1 and Mfn2 (Fig. 6C-I), were significantly decreased by the LPS treatment. Moreover, the levels of mitophagy markers, such as PINK1, Parkin, and Beclin1, were also inhibited in LPS-treated hearts, a result that was followed by an accumulation of p62, indicative of mitochondrial autophagy arrest (Fig. 6C-M). Interestingly, treatment with melatonin prevented the increase in the levels of mitochondrial fission factors and reversed the decrease in the levels of mitochondrial fusion proteins (Fig. 6C-I). In addition, mitophagy activity was also enhanced by melatonin in LPS-treated hearts (Fig. 6C-M). Notably, ad-Ripk3 transfection abolished the regulatory effects of melatonin on mitochondrial dynamics, as evidenced by increased mitochondrial fission, decreased mitochondrial fusion and inactive mitophagy (Fig. 6C-M). Taken together, our results indicate that mitochondrial dynamics are disturbed by LPS and are reversed to near-normal levels by the melatonin treatment through the suppression of Ripk3 expression.

3.7. Melatonin modifies LPS-induced ER stress and calcium imbalance in sepsis-induced cardiomyopathy

In addition to mitochondrial damage, ER stress has also been shown to be associated with the progression of septic cardiomyopathy. Western blotting analyses revealed increased levels of proteins related to ER stress, such as PERK, CHOP and GRP78, in LPS-treated mice (Fig. 7A–D), and these changes were reversed by Ripk3 deletion and/or melatonin treatment (Fig. 7A–D). Notably, the transfection of ad-Ripk3 abolished the inhibitory effects of melatonin on ER stress (Fig. 7A–D). Mechanistically, the ER is an intracellular Ca^{2+} store that primarily regulates cytosolic Ca^{2+} signaling. Accordingly, Fura-2 was used to detect alterations in cellular calcium signaling in LPS-treated cardiomyocytes. As shown in Fig. 7E–F, compared to the control group, the LPS treatment increased the cytoplasmic calcium concentrations, and this effect was negated by melatonin through the repression of Ripk3 expression (Fig. 7E–F). Thus, LPS-mediated cytoplasmic calcium overloading was reversed be melatonin.

Based on previous studies, the ER controls intracellular calcium homeostasis by modifying the expression of calcium pumps [77]. Two types of calcium pumps have been identified in the ER. One is calcium release channels, such as IP3R. The other is calcium uptake proteins, such as SERCA. Interestingly, IP3R expression was upregulated and SERCA expression was downregulated in LPS-treated hearts (Fig. 7G–I). The loss of Ripk3 and/or treatment with melatonin reversed the decrease in SERCA expression and reduced the levels of IP3R (Fig. 7G–I). Based on our results, ER stress was also activated in septic cardiomyopathy, and melatonin attenuated ER stress and subsequently reversed changes in cardiomyocyte calcium homeostasis.

3.8. Melatonin normalizes the cardioprotective signals in LPS-treated hearts by reducing Ripk3 expression

Finally, we explored the effect of melatonin on cardioprotective signaling in LPS-treated hearts. Based on previous findings, three key signaling pathways are responsible for cardioprotective signaling: AKT, ERK and AMPK. In addition, two cardiac damage signals have been shown to exacerbate myocardial injury: the JNK and Mst1 pathways. In the present study, the levels of p-AKT, p-ERK, and p-AMPK were significantly decreased in LPS-treated hearts (Fig. 8A–F). Interestingly, the melatonin treatment reversed the changes in the activity of AKT, ERK and AMPK, as evidenced by increased p-AKT, p-ERK and p-AMPK levels (Fig. 8A–F). Notably, the effects of melatonin on promoting the cardiac expression of pro-survival signals were negated by ad-Ripk3 transfection. Thus, cardioprotective signals were actually activated by melatonin in the setting of LPS-induced septic cardiomyopathy.

In contrast, the levels of p-JNK and Mst1 were rapidly increased in response to the LPS treatment (Fig. 8A–F), indicating the activation of the JNK and Mst1 pathways. However, the melatonin treatment decreased p-JNK and Mst1 levels, and these effects were negated by ad-Ripk3 transfection (Fig. 8A–F), suggesting that cardiac damage signals are inhibited by melatonin via the repression of Ripk3. This finding was also validated in cardiomyocytes using immunofluorescence staining. Compared to the control cells, LPS-treated cardiomyocytes exhibited lower levels of p-AKT and higher levels of p-JNK. Notably, melatonin mediated AKT activation and JNK inhibition in LPS-treated cells, and these alterations were neutralized by ad-Ripk3 transfection (Fig. 8G–I). Based on these results, melatonin normalized the cardioprotective signals in LPS-induced septic cardiomyopathy.

4. Discussion

LPS-induced septic cardiomyopathy is associated with mitochondrial injury, inflammatory damage and ER stress. An understanding of the molecular mechanisms of these pathogenic processes may facilitate the development of new treatment modalities for septic cardiomyopathy. In the present study, we reported that Ripk3 upregulation seemed to be a primary upstream mediator of septic cardiomyopathy. Increased Ripk3 expression impaired cardiac function, amplified the myocardial inflammatory response, and induced cardiomyocyte death. From a molecular perspective, higher Ripk3 expression promoted the degradation of the contractile cytoskeleton, induced the collapse of the mitochondrial energy metabolism, generated imbalanced mitochondrial dynamics, promoted oxidative stress, initiated ER stress, elicited cytoplasmic calcium overloading and hindered cardioprotective signals in cardiomyocytes. Interestingly, LPS-mediated cardiac dysfunction, mitochondrial injury and ER stress were prevented by a melatonin injection through a mechanism attributed to Ripk3 suppression. To our knowledge, this investigation is the first to substantiate the sufficiency of pathogenically relevant degrees of Ripk3-modified mitochondrial injury and ER stress in aggravating LPS-induced septic cardiomyopathy, as well as the necessary role for melatonin as an effective agent to prevent sepsis-induced myocardial injury.

The multiple regulatory effects of melatonin on inflammatory injury have been widely explored [78,79]. In pancreatic inflammation, a neonatal brain inflammation model, muscular inflammation damage, chronic obstructive pulmonary disease, and diabetic retinopathy, melatonin modulates the inflammatory response and attenuates tissue damage. This inflammation indicates that melatonin may be useful in fighting against sepsis due to its anti-inflammatory actions. This hypothesis is subsequently supported by several in-depth studies. For example, melatonin reduces the mortality of septic mice by disrupting the NF-κB/NLRP3 interaction, attenuating septic liver dysfunction via reversing changes in mitochondrial complex I activity [80], combatting

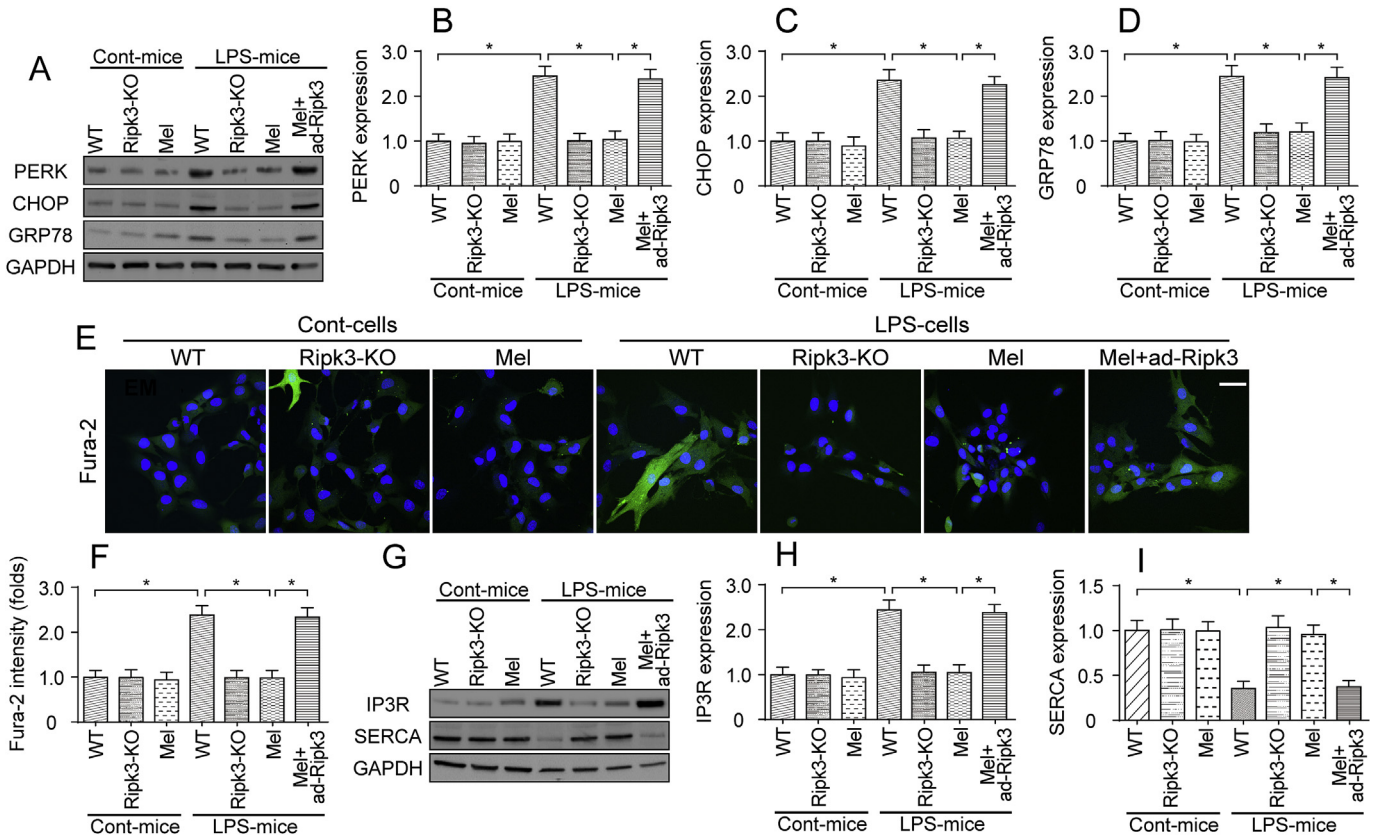

Fig. 7. LPS-induced ER stress and cytoplasmic calcium overloading were inhibited by melatonin. A-D. Cardiomyocytes were isolated from WT and Ripk3-KO mice. Then, the levels of proteins related to ER stress, such as PERK, CHOP, and GRP78, were determined using western blotting. **E-F.** Cardiomyocyte calcium concentrations was determined using Fura-2AM staining. Subsequently, the fluorescence intensity of calcium was calculated in cells treated with LPS and/or melatonin. Bar: 65 μm. **G-I.** Proteins were isolated from cardiomyocytes and then western blotting was used to observe the changes in proteins related to ER calcium homeostasis. $*p < 0.05$.

bacterial infection via preventing bacterial translocation [81], and reducing brain injury via neutralizing oxidative stress. Moreover, the beneficial effect of melatonin on septic cardiomyopathy has also been validated in many careful investigations, and the possible protective mechanisms involved include the protection of mitochondrial function, modification ER homeostasis and control of inflammation. However, the exact regulatory machinery by which melatonin exerts its protective effect and the primary molecules that fine-tune mitochondrial function and ER homeostasis remain to be elucidated. The present study identifies Ripk3 as a primary pathogenic factor that acts by amplifying mitochondrial dysfunction, ER stress and the inflammatory response, revealing a striking pattern of mutual interactions between Ripk3, the mitochondria and ER. On the other hand, from a therapeutic perspective, clinicians should remember that the therapeutic effect of melatonin is mainly ascribed to its inhibitory action on Ripk3.

In addition to Ripk3, the present study reports three novel findings. First, we reported that mitochondrial dynamics were disturbed in septic cardiomyopathy, as evidenced by increased mitochondrial fission, decreased mitochondrial fusion and inactive mitophagy. Abnormal mitochondrial dynamics were associated with mitochondria energy depletion, participating in myocardial contractile dysfunction [82]. Second, ER stress and ER-modulated cardiomyocyte calcium disturbances were also noted in LPS-induced septic cardiomyopathy. Although previous studies have reported altered ER function in inflammation-mediated myocardial injury, little evidence is available to explain the causal role of ER in LPS-induced septic cardiomyopathy. Our results demonstrated that LPS-mediated ER stress was associated with calcium overloading and calcium channel dysfunction. This finding may explain the mechanisms underlying myocardial depression in septic subjects. Third, we reported that cardiomyocyte cytoskeletal degradation also occurred in the LPS-treated hearts due to Ripk3 upregulation. In addition to maintaining the mitochondrial ATP supply and calcium homeostasis, cardiomyocytes must employ the contractile cytoskeleton to ensure heart systole and diastole. Accordingly, more attention should be paid to the regulatory mechanisms underlying the sepsis-induced disintegration of the cardiomyocyte cytoskeleton. Collectively, these three novel findings may lay the foundation to improve our understanding of the etiology of LPS-induced septic cardiomyopathy.

More importantly, our results provided ample data to support the use of melatonin as an effective and practical treatment to attenuate septic myocardial injury. At the molecular level, the melatonin treatment reversed changes in mitochondrial dynamics, ameliorated ER stress and prevented the disassembly of the cardiomyocyte cytoskeleton by repressing Ripk3. This study is the first to comprehensively report the multiple impacts of melatonin on the mitochondria, ER and cardiomyocyte cytoskeleton. Therefore, it is necessary to point out that our data also provide new evidence to explain the defensive role of melatonin in sepsis-induced myocardial depression.

There are several limitations in the present study. First, an ad-Ripk3 injection was used to overexpress Ripk3 in the myocardium. However, a better method would be to apply Ripk3 transgenic mice for the rescue experiments of Ripk3. Second, little is known about the mechanisms by which melatonin represses Ripk3 expression. Additional investigations are required to verify whether melatonin transcriptionally and/or post-transcriptionally affected the stability of Ripk3 following LPS challenge. Third, melatonin is a kind of antioxidant and the ROS suppressive effect of melatonin contributes to cardiomyocyte survival in the setting of

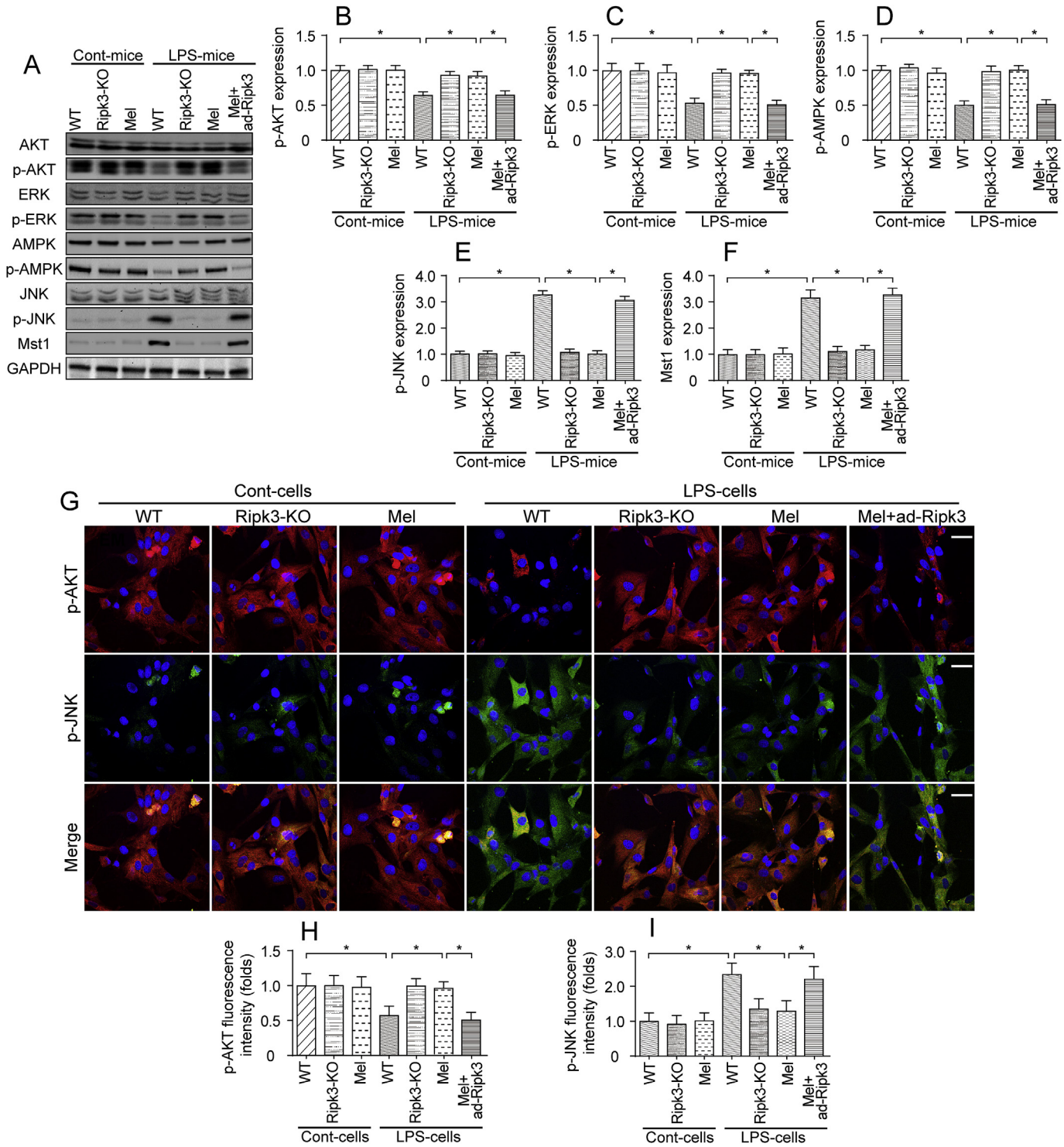

Fig. 8. Cardioprotective signaling pathways were modulated by melatonin in the setting of LPS-mediated myocardial injury. A-F. Proteins were isolated from heart tissues and the levels of p-AKT, p-ERK, p-AMPK, p-JNK, and Mst1 were determined. The cardioprotective signaling pathway includes p-AKT, p-ERK, and p-AMPK. However, p-JNK and Mst1 are related to cardiac damage and their levels were also measured using western blotting. **G-I.** Immunofluorescence staining for p-AKT and p-JNK in cardiomyocytes treated with LPS and melatonin. The immunofluorescence intensity of p-JNK and p-AKT was determined. Bar: 85 μm $^*p < 0.05$.

sepsis-induced myocardial depression. However, there are several other antioxidants molecules and thus more studies are necessary to further compare the therapeutic effects of melatonin and other antioxidant factors in septic cardiomyopathy.

Conflicts of interest

The authors have declared that they have no conflict of interests.

Acknowledgements

This work is funded by National Natural Science Foundation Youth

Program of China (NO: 81700388), Natural Science Foundation of Guangdong Province of China (NO: 2018A030313067), the Major Scientific Research Foundation of Colleges and Universities of Guangdong Province (NO: 2016KZDXM016), the Clinical Training Foundation of Southern Medical University (NO: LC2016PY002), Science and Technology Innovation Project from Foshan, Guangdong (NO: FS0AA-KJ218-1301-0006; FS0AA-KJ218-1301-0010) and Key Specialist Department Training Project of Foshan City, Guangdong Province of China (No: FSPY3-2015034).

References

[1] E. Aanhane, I.A. Schulkens, R. Heusschen, K. Castricum, H. Leffler, A.W. Griffioen, V.L. Thijssen, Different angioregulatory activity of monovalent galectin-9 isoforms, Angiogenesis 21 (3) (2018) 545–555.
[2] Y. Abukar, R. Ramchandra, S.G. Hood, M.J. Mckinley, L.C. Booth, S.T. Yao, C.N. May, Increased cardiac sympathetic nerve activity in ovine heart failure is reduced by lesion of the area postrema, but not lamina terminalis, Basic Res. Cardiol. 113 (5) (2018) 35.
[3] R.G. Abeysuriya, S.W. Lockley, P.A. Robinson, S. Postnova, A unified model of melatonin, 6-sulfatoxymelatonin, and sleep dynamics, J. Pineal Res. 64 (4) (2018) e12474.
[4] P.R. Angelova, M. Barilani, C. Lovejoy, M. Dossena, M. Vigano, A. Seresini, D. Piga, S. Gandhi, G. Pezzoli, A.Y. Abramov, L. Lazzari, Mitochondrial dysfunction in Parkinsonian mesenchymal stem cells impairs differentiation, Redox Biol 14 (2018) 474–484.
[5] J.F. Frencken, D.W. Donker, C. Spitoni, M.E. Koster-Brouwer, I.W. Soliman, D.S.Y. Ong, J. Horn, T. Van Der Poll, W.A. Van Klei, M.J.M. Bonten, O.L. Cremer, Myocardial injury in patients with sepsis and its association with long-term outcome, Circ Cardiovasc Qual Outcomes 11 (2) (2018) e004040.
[6] M.B. Afonso, P.M. Rodrigues, A.L. Simao, M.M. Gaspar, T. Carvalho, P. Borralho, J.M. Banales, R.E. Castro, C.M.P. Rodrigues, miRNA-21 ablation protects against liver injury and necroptosis in cholestasis, Cell Death Differ. 25 (5) (2018) 857–872.
[7] M. Araki, T. Hisamitsu, Y. Kinugasa-Katayama, T. Tanaka, Y. Harada, S. Nakao, S. Hanada, S. Ishii, M. Fujita, T. Kawamura, Y. Saito, K. Nishiyama, Y. Watanabe, O. Nakagawa, Serum/glucocorticoid-regulated kinase 1 as a novel transcriptional target of bone morphogenetic protein-ALK1 receptor signaling in vascular endothelial cells, Angiogenesis 21 (2) (2018) 415–423.
[8] H.E. Botker, D. Hausenloy, I. Andreadou, S. Antonucci, K. Boengler, S.M. Davidson, S. Deshwal, Y. Devaux, F. Di Lisa, M. Di Sante, P. Efentakis, S. Femmino, D. Garcia-Dorado, Z. Giricz, B. Ibanez, E. Iliodromitis, N. Kaludercic, P. Kleinbongard, M. Neuhauser, M. Ovize, P. Pagliaro, M. Rahbek-Schmidt, M. Ruiz-Meana, K.D. Schluter, R. Schulz, A. Skyschally, C. Wilder, D.M. Yellon, P. Ferdinandy, G. Heusch, Practical guidelines for rigor and reproducibility in preclinical and clinical studies on cardioprotection, Basic Res. Cardiol. 113 (5) (2018) 39.
[9] M. Alvarez-Fernandez, M. Sanz-Flores, B. Sanz-Castillo, M. Salazar-Roa, D. Partida, E. Zapatero-Solana, H.R. Ali, E. Manchado, S. Lowe, T. Vanarsdale, D. Shields, C. Caldas, M. Quintela-Fandino, M. Malumbres, Therapeutic relevance of the PP2A-B55 inhibitory kinase MASTL/Greatwall in breast cancer, Cell Death Differ. 25 (5) (2018) 828–840.
[10] A. Durand, T. Duburcq, T. Dekeyser, R. Neviere, M. Howsam, R. Favory, S. Preau, Involvement of mitochondrial disorders in septic cardiomyopathy, Oxid Med Cell Longev (2017) 4076348 2017.
[11] J.A. Boga, B. Caballero, Y. Potes, Z. Perez-Martinez, R.J. Reiter, I. Vega-Naredo, A. Coto-Montes, Therapeutic potential of melatonin related to its role as an autophagy regulator: a review, J. Pineal Res. (2018) e12534.
[12] V. Brazao, R.P. Colato, F.H. Santello, G.T.D. Vale, N.A. Gonzaga, C.R. Tirapelli, J.C.D. Prado Jr., Effects of melatonin on thymic and oxidative stress dysfunctions during Trypanosoma cruzi infection, J. Pineal Res. 65 (3) (2018) e12510.
[13] H. Zhou, S. Wang, S. Hu, Y. Chen, J. Ren, ER-mitochondria microdomains in cardiac ischemia-reperfusion injury: a fresh perspective, Front. Physiol. 9 (2018) 755.
[14] X. Ba, I. Boldogh, 8-Oxoguanine DNA glycosylase 1: beyond repair of the oxidatively modified base lesions, Redox Biol 14 (2018) 669–678.
[15] X.Z. Zhuo, Y. Wu, Y.J. Ni, J.H. Liu, M. Gong, X.H. Wang, F. Wei, T.Z. Wang, Z. Yuan, A.Q. Ma, P. Song, Isoproterenol instigates cardiomyocyte apoptosis and heart failure via AMPK inactivation-mediated endoplasmic reticulum stress, Apoptosis 18 (7) (2013) 800–810.
[16] E.D. Coverstone, R.G. Bach, L. Chen, L.J. Bierut, A.Y. Li, P.A. Lenzini, H.C. O'neill, J.A. Spertus, C.C. Sucharov, J.A. Stitzel, J.D. Schilling, S. Cresci, A novel genetic marker of decreased inflammation and improved survival after acute myocardial infarction, Basic Res. Cardiol. 113 (5) (2018) 38.
[17] N. Armartmuntree, M. Murata, A. Techasen, P. Yongvanit, W. Loilome, N. Namwat, C. Pairojkul, C. Sakonsinsiri, S. Pinlaor, R. Thanan, Prolonged oxidative stress down-regulates Early B cell factor 1 with inhibition of its tumor suppressive function against cholangiocarcinoma genesis, Redox Biol 14 (2018) 637–644.
[18] A.M. Crist, A.R. Lee, N.R. Patel, D.E. Westhoff, S.M. Meadows, Vascular deficiency of Smad4 causes arteriovenous malformations: a mouse model of Hereditary Hemorrhagic Telangiectasia, Angiogenesis 21 (2) (2018) 363–380.
[19] A. Bagati, A. Bianchi-Smiraglia, S. Moparthy, K. Kolesnikova, E.E. Fink, M. Kolesnikova, M.V. Roll, P. Jowdy, D.W. Wolff, A. Polechetti, D.H. Yun, B.C. Lipchick, L.M. Paul, B. Wrazen, K. Moparthy, S. Mudambi, G.E. Morozevich, S.G. Georgieva, J. Wang, G. Shafirstein, S. Liu, E.S. Kandel, A.E. Berman, N.F. Box, G. Paragh, M.A. Nikiforov, FOXQ1 controls the induced differentiation of melanocytic cells, Cell Death Differ. 25 (6) (2018) 1040–1049.
[20] L. a. E. Erland, M.R. Shukla, A.S. Singh, S.J. Murch, P.K. Saxena, Melatonin and serotonin: mediators in the symphony of plant morphogenesis, J. Pineal Res. 64 (2) (2018).
[21] A. Sureshbabu, E. Patino, K.C. Ma, K. Laursen, E.J. Finkelsztein, O. Akchurin, T. Muthukumar, S.W. Ryter, L. Gudas, A.M.K. Choi, M.E. Choi, RIPK3 promotes sepsis-induced acute kidney injury via mitochondrial dysfunction, JCI Insight 3 (11) (2018).
[22] H. Zhou, D. Li, P. Zhu, Q. Ma, S. Toan, J. Wang, S. Hu, Y. Chen, Y. Zhang, Inhibitory effect of melatonin on necroptosis via repressing the Ripk3-PGAM5-CypD-mPTP pathway attenuates cardiac microvascular ischemia-reperfusion injury, J. Pineal Res. 65 (3) (2018) e12503.
[23] M. Biernacki, E. Ambrozewicz, A. Gegotek, M. Toczek, K. Bielawska, E. Skrzydlewska, Redox system and phospholipid metabolism in the kidney of hypertensive rats after FAAH inhibitor URB597 administration, Redox Biol 15 (2018) 41–50.
[24] E. Daniel, D.B. Azizoglu, A.R. Ryan, T.A. Walji, C.P. Chaney, G.I. Sutton, T.J. Carroll, D.K. Marciano, O. Cleaver, Spatiotemporal heterogeneity and patterning of developing renal blood vessels, Angiogenesis 21 (3) (2018) 617–634.
[25] S.M. Davidson, S. Arjun, M.V. Basalay, R.M. Bell, D.I. Bromage, H.E. Botker, R.D. Carr, J. Cunningham, A.K. Ghosh, G. Heusch, B. Ibanez, P. Kleinbongard, S. Lecour, H. Maddock, M. Ovize, M. Walker, M. Wiart, D.M. Yellon, The 10th Biennial Hatter Cardiovascular Institute workshop: cellular protection-evaluating new directions in the setting of myocardial infarction, ischaemic stroke, and cardio-oncology, Basic Res. Cardiol. 113 (6) (2018) 43.
[26] L. Cabon, A. Bertaux, M.N. Brunelle-Navas, I. Nemazanyy, L. Scourzic, L. Delavallee, L. Vela, M. Baritaud, S. Bouchet, C. Lopez, V. Quang Van, K. Garbin, D. Chateau, F. Gilard, M. Sarfati, T. Mercher, O.A. Bernard, S.A. Susin, AIF loss deregulates hematopoiesis and reveals different adaptive metabolic responses in bone marrow cells and thymocytes, Cell Death Differ. 25 (5) (2018) 983–1001.
[27] L. a. E. Erland, A. Yasunaga, I.T.S. Li, S.J. Murch, P.K. Saxena, Direct visualization of location and uptake of applied melatonin and serotonin in living tissues and their redistribution in plants in response to thermal stress, J. Pineal Res. (2018) e12527.
[28] M. Ding, J. Ning, N. Feng, Z. Li, Z. Liu, Y. Wang, Y. Wang, X. Li, C. Huo, X. Jia, R. Xu, F. Fu, X. Wang, J. Pei, Dynamin-related protein 1-mediated mitochondrial fission contributes to post-traumatic cardiac dysfunction in rats and the protective effect of melatonin, J. Pineal Res. 64 (1) (2018).
[29] H. Zhou, Y. Zhang, S. Hu, C. Shi, P. Zhu, Q. Ma, Q. Jin, F. Cao, F. Tian, Y. Chen, Melatonin protects cardiac microvasculature against ischemia/reperfusion injury via suppression of mitochondrial fission-VDAC1-HK2-mPTP-mitophagy axis, J. Pineal Res. 63 (1) (2017).
[30] H. Zhou, Q. Ma, P. Zhu, J. Ren, R.J. Reiter, Y. Chen, Protective role of melatonin in cardiac ischemia-reperfusion injury: from pathogenesis to targeted therapy, J. Pineal Res. 64 (3) (2018).
[31] H. Zhou, W. Du, Y. Li, C. Shi, N. Hu, S. Ma, W. Wang, J. Ren, Effects of melatonin on fatty liver disease: the role of NR4A1/DNA-PKcs/p53 pathway, mitochondrial fission, and mitophagy, J. Pineal Res. 64 (1) (2018).
[32] C. Bellomo, L. Caja, I. Fabregat, W. Mikulits, D. Kardassis, C.H. Heldin, A. Moustakas, Snail mediates crosstalk between TGFbeta and LXRalpha in hepatocellular carcinoma, Cell Death Differ. 25 (5) (2018) 885–903.
[33] K. Drosatos, R.S. Khan, C.M. Trent, H. Jiang, N.H. Son, W.S. Blaner, S. Homma, P.C. Schulze, I.J. Goldberg, Peroxisome proliferator-activated receptor-gamma activation prevents sepsis-related cardiac dysfunction and mortality in mice, Circ Heart Fail 6 (3) (2013) 550–562.
[34] J. Chen, B. Wang, J. Lai, Z. Braunstein, M. He, G. Ruan, Z. Yin, J. Wang, K. Cianflone, Q. Ning, C. Chen, D.W. Wang, Trimetazidine attenuates cardiac dysfunction in endotoxemia and sepsis by promoting neutrophil migration, Front. Immunol. 9 (2018) 2015.
[35] M. Fukumoto, K. Kondo, K. Uni, T. Ishiguro, M. Hayashi, S. Ueda, I. Mori, K. Niimi, F. Tashiro, S. Miyazaki, J.I. Miyazaki, S. Inagaki, T. Furuyama, Tip-cell behavior is regulated by transcription factor FoxO1 under hypoxic conditions in developing mouse retinas, Angiogenesis 21 (2) (2018) 203–214.
[36] G. Farber, R. Hurtado, S. Loh, S. Monette, J. Mtui, R. Kopan, S. Quaggin, C. Meyer-Schwesinger, D. Herzlinger, R.P. Scott, C.P. Blobel, Glomerular endothelial cell maturation depends on ADAM10, a key regulator of Notch signaling, Angiogenesis 21 (2) (2018) 335–347.
[37] M. Chandra, D. Escalante-Alcalde, M.S. Bhuiyan, A.W. Orr, C. Kevil, A.J. Morris, H. Nam, P. Dominic, K.J. Mccarthy, S. Miriyala, M. Panchatcharam, Cardiac-specific inactivation of LPP3 in mice leads to myocardial dysfunction and heart failure, Redox Biol 14 (2018) 261–271.
[38] A. Care, M. Bellenghi, P. Matarrese, L. Gabriele, S. Salvioli, W. Malorni, Sex disparity in cancer: roles of microRNAs and related functional players, Cell Death Differ. 25 (3) (2018) 477–485.
[39] K.S. Edwards, S. Ashraf, T.M. Lomax, J.M. Wiseman, M.E. Hall, F.N. Gava, J.E. Hall, J.P. Hosler, R. Harmancey, Uncoupling protein 3 deficiency impairs myocardial fatty acid oxidation and contractile recovery following ischemia/reperfusion, Basic Res. Cardiol. 113 (6) (2018) 47.
[40] Q. Jin, R. Li, N. Hu, T. Xin, P. Zhu, S. Hu, S. Ma, H. Zhu, J. Ren, H. Zhou, DUSP1 alleviates cardiac ischemia/reperfusion injury by suppressing the Mff-required mitochondrial fission and Bnip3-related mitophagy via the JNK pathways, Redox Biol 14 (2018) 576–587.
[41] A. Deussen, Mechanisms underlying coronary autoregulation continue to await clarification, Basic Res. Cardiol. 113 (5) (2018) 34.
[42] T. Chen, S.H. Dai, X. Li, P. Luo, J. Zhu, Y.H. Wang, Z. Fei, X.F. Jiang, Sirt1-Sirt3 axis regulates human blood-brain barrier permeability in response to ischemia, Redox

Biol 14 (2018) 229–236.
[43] R. Hardeland, Melatonin and inflammation-Story of a double-edged blade, J. Pineal Res. 65 (4) (2018) e12525.
[44] A. Galano, R.J. Reiter, Melatonin and its metabolites vs oxidative stress: from individual actions to collective protection, J. Pineal Res. 65 (1) (2018) e12514.
[45] N.R. Gonzalez, R. Liou, F. Kurth, H. Jiang, J. Saver, Antiangiogenesis and medical therapy failure in intracranial atherosclerosis, Angiogenesis 21 (1) (2018) 23–35.
[46] E. Cremonini, Z. Wang, A. Bettaieb, A.M. Adamo, E. Daveri, D.A. Mills, K.M. Kalanetra, F.G. Haj, S. Karakas, P.I. Oteiza, (-)-Epicatechin protects the intestinal barrier from high fat diet-induced permeabilization: implications for steatosis and insulin resistance, Redox Biol 14 (2018) 588–599.
[47] M.M. Cortese-Krott, E. Mergia, C.M. Kramer, W. Luckstadt, J. Yang, G. Wolff, C. Panknin, T. Bracht, B. Sitek, J. Pernow, J.P. Stasch, M. Feelisch, D. Koesling, M. Kelm, Identification of a soluble guanylate cyclase in RBCs: preserved activity in patients with coronary artery disease, Redox Biol 14 (2018) 328–337.
[48] C.C. Huang, H.M. Kuo, P.C. Wu, S.H. Cheng, T.T. Chang, Y.C. Chang, M.L. Kung, D.C. Wu, J.H. Chuang, M.H. Tai, Soluble delta-like 1 homolog (DLK1) stimulates angiogenesis through Notch1/Akt/eNOS signaling in endothelial cells, Angiogenesis 21 (2) (2018) 299–312.
[49] A. Kazakov, R.A. Hall, C. Werner, T. Meier, A. Trouvain, S. Rodionycheva, A. Nickel, F. Lammert, C. Maack, M. Bohm, U. Laufs, Raf kinase inhibitor protein mediates myocardial fibrosis under conditions of enhanced myocardial oxidative stress, Basic Res. Cardiol. 113 (6) (2018) 42.
[50] H. Chen, M.W. Kankel, S.C. Su, S.W.S. Han, D. Ofengeim, Exploring the genetics and non-cell autonomous mechanisms underlying ALS/FTLD, Cell Death Differ. 25 (4) (2018) 646–660.
[51] R. Jeelani, D. Maitra, C. Chatzicharalampous, S. Najeemuddin, R.T. Morris, H.M. Abu-Soud, Melatonin prevents hypochlorous acid-mediated cyanocobalamin destruction and cyanogen chloride generation, J. Pineal Res. 64 (3) (2018).
[52] J.R. Frandsen, P. Narayanasamy, Neuroprotection through flavonoid: enhancement of the glyoxalase pathway, Redox Biol 14 (2018) 465–473.
[53] F. Jin, N. Hagemann, L. Sun, J. Wu, T.R. Doeppner, Y. Dai, D.M. Hermann, High-density lipoprotein (HDL) promotes angiogenesis via S1P3-dependent VEGFR2 activation, Angiogenesis 21 (2) (2018) 381–394.
[54] P. Mehra, Y. Guo, Y. Nong, P. Lorkiewicz, M. Nasr, Q. Li, S. Muthusamy, J.A. Bradley, A. Bhatnagar, M. Wysoczynski, R. Bolli, B.G. Hill, Cardiac mesenchymal cells from diabetic mice are ineffective for cell therapy-mediated myocardial repair, Basic Res. Cardiol. 113 (6) (2018) 46.
[55] C. Korbel, M.D. Gerstner, M.D. Menger, M.W. Laschke, Notch signaling controls sprouting angiogenesis of endometriotic lesions, Angiogenesis 21 (1) (2018) 37–46.
[56] J. Merz, P. Albrecht, S. Von Garlen, I. Ahmed, D. Dimanski, D. Wolf, I. Hilgendorf, C. Hardtner, K. Grotius, F. Willecke, T. Heidt, H. Bugger, N. Hoppe, U. Kintscher, C. Von Zur Muhlen, M. Idzko, C. Bode, A. Zirlik, P. Stachon, Purinergic receptor Y2 (P2Y2)- dependent VCAM-1 expression promotes immune cell infiltration in metabolic syndrome, Basic Res. Cardiol. 113 (6) (2018) 45.
[57] A. Lochner, E. Marais, B. Huisamen, Melatonin and cardioprotection against ischaemia/reperfusion injury: what's new? A review, J. Pineal Res. 65 (1) (2018) e12490.
[58] H. Zhou, Y. Yue, J. Wang, Q. Ma, Y. Chen, Melatonin therapy for diabetic cardiomyopathy: a mechanism involving Syk-mitochondrial complex I-SERCA pathway, Cell. Signal. 47 (2018) 88–100.
[59] S. Owino, A. Sanchez-Bretano, C. Tchio, E. Cecon, A. Karamitri, J. Dam, R. Jockers, G. Piccione, H.L. Noh, T. Kim, J.K. Kim, K. Baba, G. Tosini, Nocturnal activation of melatonin receptor type 1 signaling modulates diurnal insulin sensitivity via regulation of PI3K activity, J. Pineal Res. 64 (3) (2018).
[60] L. Hao, Q. Sun, W. Zhong, W. Zhang, X. Sun, Z. Zhou, Mitochondria-targeted ubiquinone (MitoQ) enhances acetaldehyde clearance by reversing alcohol-induced posttranslational modification of aldehyde dehydrogenase 2: a molecular mechanism of protection against alcoholic liver disease, Redox Biol 14 (2018) 626–636.
[61] M. Serocki, S. Bartoszewska, A. Janaszak-Jasiecka, R.J. Ochocka, J.F. Collawn, R. Bartoszewski, miRNAs regulate the HIF switch during hypoxia: a novel therapeutic target, Angiogenesis 21 (2) (2018) 183–202.
[62] R. Li, T. Xin, D. Li, C. Wang, H. Zhu, H. Zhou, Therapeutic effect of Sirtuin 3 on ameliorating nonalcoholic fatty liver disease: the role of the ERK-CREB pathway and Bnip3-mediated mitophagy, Redox Biol 18 (2018) 229–243.
[63] D. Henderson, C. Huebner, M. Markowitz, N. Taube, Z.M. Harvanek, U. Jakob, D. Knoefler, Do developmental temperatures affect redox level and lifespan in C. elegans through upregulation of peroxiredoxin? Redox Biol 14 (2018) 386–390.
[64] K.M. Thieltges, D. Avramovic, C.L. Piscitelli, S. Markovic-Mueller, H.K. Binz, K. Ballmer-Hofer, Characterization of a drug-targetable allosteric site regulating vascular endothelial growth factor signaling, Angiogenesis 21 (3) (2018) 533–543.
[65] H. Zhou, N. Li, Y. Yuan, Y.G. Jin, H. Guo, W. Deng, Q.Z. Tang, Activating transcription factor 3 in cardiovascular diseases: a potential therapeutic target, Basic Res. Cardiol. 113 (5) (2018) 37.
[66] C. Hockings, A.E. Alsop, S.C. Fennell, E.F. Lee, W.D. Fairlie, G. Dewson, R.M. Kluck, Mcl-1 and Bcl-xL sequestration of Bak confers differential resistance to BH3-only proteins, Cell Death Differ. 25 (4) (2018) 719–732.
[67] J. Hasna, F. Hague, L. Rodat-Despoix, D. Geerts, C. Leroy, D. Tulasne, H. Ouadid-Ahidouch, P. Kischel, Orai3 calcium channel and resistance to chemotherapy in breast cancer cells: the p53 connection, Cell Death Differ. 25 (4) (2018) 691–705.
[68] Y. Wei, Y. Chang, H. Zeng, G. Liu, C. He, H. Shi, RAV transcription factors are essential for disease resistance against cassava bacterial blight via activation of melatonin biosynthesis genes, J. Pineal Res. 64 (1) (2018).
[69] M. Ikeda, Y. Ishima, R. Kinoshita, V.T.G. Chuang, N. Tasaka, N. Matsuo, H. Watanabe, T. Shimizu, T. Ishida, M. Otagiri, T. Maruyama, A novel S-sulfhydrated human serum albumin preparation suppresses melanin synthesis, Redox Biol 14 (2018) 354–360.
[70] H. Zhou, S. Wang, P. Zhu, S. Hu, Y. Chen, J. Ren, Empagliflozin rescues diabetic myocardial microvascular injury via AMPK-mediated inhibition of mitochondrial fission, Redox Biol 15 (2018) 335–346.
[71] H. Zhou, P. Zhu, J. Guo, N. Hu, S. Wang, D. Li, S. Hu, J. Ren, F. Cao, Y. Chen, Ripk3 induces mitochondrial apoptosis via inhibition of FUNDC1 mitophagy in cardiac IR injury, Redox Biol 13 (2017) 498–507.
[72] P. Zhu, S. Hu, Q. Jin, D. Li, F. Tian, S. Toan, Y. Li, H. Zhou, Y. Chen, Ripk3 promotes ER stress-induced necroptosis in cardiac IR injury: a mechanism involving calcium overload/XO/ROS/mPTP pathway, Redox Biol 16 (2018) 157–168.
[73] H. Zhu, Q. Jin, Y. Li, Q. Ma, J. Wang, D. Li, H. Zhou, Y. Chen, Melatonin protected cardiac microvascular endothelial cells against oxidative stress injury via suppression of IP3R-[Ca(2+)]c/VDAC-[Ca(2+)]m axis by activation of MAPK/ERK signaling pathway, Cell Stress Chaperones 23 (1) (2018) 101–113.
[74] H. Zhou, S. Hu, Q. Jin, C. Shi, Y. Zhang, P. Zhu, Q. Ma, F. Tian, Y. Chen, Mff-dependent mitochondrial fission contributes to the pathogenesis of cardiac microvasculature ischemia/reperfusion injury via induction of mROS-mediated cardiolipin oxidation and HK2/VDAC1 disassociation-involved mPTP opening, J Am Heart Assoc 6 (3) (2017).
[75] H. Zhou, J. Wang, S. Hu, H. Zhu, S. Toanc, J. Ren, BI1 alleviates cardiac microvascular ischemia-reperfusion injury via modifying mitochondrial fission and inhibiting XO/ROS/F-actin pathways, J. Cell. Physiol. 234 (4) (2019) 5056–5069.
[76] H. Zhou, P. Zhu, J. Wang, H. Zhu, J. Ren, Y. Chen, Pathogenesis of cardiac ischemia reperfusion injury is associated with CK2alpha-disturbed mitochondrial homeostasis via suppression of FUNDC1-related mitophagy, Cell Death Differ. 25 (6) (2018) 1080–1093.
[77] H. Zhou, J. Wang, P. Zhu, S. Hu, J. Ren, Ripk3 regulates cardiac microvascular reperfusion injury: the role of IP3R-dependent calcium overload, XO-mediated oxidative stress and F-action/filopodia-based cellular migration, Cell. Signal. 45 (2018) 12–22.
[78] C. Riehle, J. Bauersachs, Of mice and men: models and mechanisms of diabetic cardiomyopathy, Basic Res. Cardiol. 114 (1) (2018) 2.
[79] R. Jain, J.D. Mintern, I. Tan, G. Dewson, A. Strasser, D.H.D. Gray, How do thymic epithelial cells die? Cell Death Differ. 25 (5) (2018) 1002–1004.
[80] H. Zhou, J. Wang, P. Zhu, H. Zhu, S. Toan, S. Hu, J. Ren, Y. Chen, NR4A1 aggravates the cardiac microvascular ischemia reperfusion injury through suppressing FUNDC1-mediated mitophagy and promoting Mff-required mitochondrial fission by CK2alpha, Basic Res. Cardiol. 113 (4) (2018) 23.
[81] J.B.T. Moore, X.L. Tang, J. Zhao, A.G. Fischer, W.J. Wu, S. Uchida, A.M. Gumpert, H. Stowers, M. Wysoczynski, R. Bolli, Epigenetically modified cardiac mesenchymal stromal cells limit myocardial fibrosis and promote functional recovery in a model of chronic ischemic cardiomyopathy, Basic Res. Cardiol. 114 (1) (2018) 3.
[82] H. Zhou, C. Shi, S. Hu, H. Zhu, J. Ren, Y. Chen, BI1 is associated with microvascular protection in cardiac ischemia reperfusion injury via repressing Syk-Nox2-Drp1-mitochondrial fission pathways, Angiogenesis 21 (3) (2018) 599–615.